https://doi.org/10.5194/gmd-2020-365
Preprint. Discussion started: 14 December 2020

Geoscientific Model Development
Discussions
Open Access

# Addressing Biases in Arctic-Boreal Carbon Cycling in the Community Land Model Version 5

Leah Birch[1], Christopher R. Schwalm[1], Sue Natali[1], Danica Lombardozzi [2], Gretchen Keppel-Aleks[3], Jennifer Watts[1], Xin Lin[3], Donatella Zona[4], Walter Oechel[4], Torsten Sachs[5], Thomas Andrew Black[6], and Brendan M. Rogers[1]

[1]Woodwell Climate Research Center
[2]National Center for Atmospheric Research
[3]University of Michigan
[4]San Diego State University
[5]GFZ German Research Centre for Geosciences
[6]University of BC

**Correspondence:** Leah Birch (lbirch@woodwellclimate.org) and Brendan Rogers (brogers@woodwellclimate.org)

**Abstract.** The Arctic-boreal zone (ABZ) is experiencing amplified warming, actively changing biogeochemical cycling of vegetation and soils. The land-to-atmosphere fluxes of $CO_2$ in the ABZ have the potential to increase in magnitude and feedback to the climate causing additional large scale warming. The ability to model and predict this vulnerability is critical to preparation for a warming world, but Earth system models have biases that may hinder understanding the rapidly changing ABZ carbon fluxes. Here we investigate circumpolar carbon cycling represented by the Community Land Model 5 (CLM5.0) with a focus on seasonal gross primary productivity (GPP) in plant functional types (PFTs). We benchmark model results using data from satellite remote sensing products and eddy covariance towers. We find consistent biases in CLM5.0 relative to observational constraints: (1) the onset of deciduous plant productivity to be late, (2) the offset of productivity to lag and remain abnormally high for all PFTs in fall, (3) a high bias of grass, shrub, and needleleaf evergreen tree productivity, and (4) an underestimation of productivity of deciduous trees. Based on these biases, we focus model development of alternate phenology, photosynthesis schemes, and carbon allocation parameters at eddy covariance tower sites. Although our improvements are focused on productivity, our final Model Recommendation results in other component $CO_2$ fluxes, e.g. Net Ecosystem Exchange (NEE) and Terrestrial Ecosystem Respiration (TER), that are more consistent with observations. Results suggest that algorithms developed for lower latitudes and more temperate environments can be inaccurate when extrapolated to the ABZ, and that many land surface models may not accurately represent carbon cycling and its recent rapid changes in high latitude ecosystems, especially when analyzed by individual PFTs.

## 1 Introduction

As the atmospheric concentration of $CO_2$ continues to rise, the Arctic-boreal Zone (ABZ) is expected to continue to warm more rapidly than the rest of the globe (Serreze and Francis, 2006; Serreze and Barry, 2011). The impacts of this accelerated warming are manifest across all major components of the ABZ — the cryosphere, hydrosphere, and biosphere (Duncan et al., 2020). The multifaceted ABZ response to warming includes accelerated carbon cycling (Jeong et al., 2018), permafrost thaw, intensification of disturbance regimes (Alexander and Mack, 2016), changes in snow cover and ecosystem water availability (Callaghan et al., 2011; Biancamaria et al., 2011), and shifts in vegetation structure and composition (Beck et al., 2011; Forkel et al., 2016; Searle and Chen, 2017). These changes in the whole ABZ terrestrial ecosystem structure and function have important implications for global climate, given the region's strong biophysical coupling (Bonan et al., 1992; Bala et al., 2007; Rogers et al., 2013, 2015) and large, and potentially vulnerable, reservoirs of below and aboveground carbon, especially in the permafrost zone (Shaver et al., 1992; McGuire et al., 2009, 2010; Koven et al., 2015; Parazoo et al., 2018; Natali et al., 2019; McGuire et al., 2018).

The responses of carbon cycling in the ABZ to changes in global climate are complex, interconnected, and may have compensating effects (Welp et al., 2016). For example, air and soil warming, in conjunction with a lengthening of the annual non-frozen period across the ABZ (Kim et al., 2012), stimulate plant productivity directly and indirectly through increased nutrient and water availability (Natali et al., 2014; Salmon et al., 2016). Warming and $CO_2$ fertilization have contributed to widespread "greening" across the ABZ, including shrubification (Myers-Smith et al., 2011, 2015) and northward treeline expansion (Lloyd and Fastie, 2003; Chapin et al., 2005), i.e. the encroachment of trees and shrubs into tundra regions. However, rapid warming across much of the ABZ is also accelerating decomposition, causing drought stress in warmer and drier landscapes (Carroll et al., 2011; Walker and Johnstone, 2014; Walker et al., 2015; Carroll and Loboda, 2017), and intensifying disturbance regimes such as wildfire and insect outbreaks (Turetsky et al., 2011; Kasischke et al., 2010; Rogers et al., 2018; Hanes et al., 2019); all of which contribute to the increasingly observed patterns of "browning" in the ABZ (Verbyla, 2011; Elmendorf et al., 2012; Phoenix and Bjerke, 2016).

As an emergent property of global change drivers in the ABZ, the seasonal cycle of $CO_2$ exchange across the ABZ has been experiencing changes in timing and magnitude of fluxes. Most critically regarding the magnitude of carbon fluxes, the atmospheric $CO_2$ concentration in the ABZ has been measured to be increasing between 30-60% during the last 60 years (Keeling et al., 1996; Randerson et al., 1999; Graven et al., 2013; Liptak et al., 2017; Jeong et al., 2018). Our current knowledge of the ABZ seasonal cycle of $CO_2$ suggests that much of the observed change in seasonal amplitude is due to increased vegetation productivity during the growing season, a result of $CO_2$ fertilization and warming (Forkel et al., 2016; Ito et al., 2016; Zhao et al., 2016). At the same time, fall and winter respiration constitute a large portion of the annual $CO_2$ budget (Euskirchen et al., 2014; Natali et al., 2019) and have been increasing with climate change (Belshe et al., 2012; Piao et al., 2008), making the implications for net sink-source dynamics uncertain (Ciais et al., 1995; McGuire et al., 2018). Hence, the current and anticipated state of carbon source-sink dynamics remains an open question in part due to the uncertainty in the dominant mechanisms and differential responses governing carbon fluxes across the ABZ.

Ground observations, satellite products, and process-based climate models are all used to understand interactions and feedbacks between changing environmental conditions and carbon cycling in the ABZ. *In situ* observations of carbon fluxes are required for mechanistic understanding but are often limited across time and space, especially in large and remote regions with extreme temperatures, like the ABZ (Virkkala et al., 2018, 2019). For example, respiration during the winter has long been assumed to be effectively zero, but better technology has slowly allowed the seasonal cycle story to grow (Natali et al., 2019).

https://doi.org/10.5194/gmd-2020-365
Preprint. Discussion started: 14 December 2020

Satellite observations provide near complete coverage in space and time, but are indirect observations of ecosystem properties, are challenged in the ABZ due to low insolation in the winter months, and contain a variety of uncertainties related to sensor properties, atmospheric contamination, and processing (Duncan et al., 2020). The brevity of the growing season and lack of light in the ABZ throughout the year also contributes to biases in satellite measurements (Randerson et al., 1997). Process-based models, or terrestrial biosphere models (TBMs), are a particularly invaluable resource for examining mechanisms across spatial and temporal scales, even projecting carbon cycle feedbacks in the future under varying socioeconomic scenarios (Taylor et al., 2012; Eyring et al., 2016, CMIP5 and 6). However, due to different formulations, assumptions, mechanisms, model inputs, and parameterizations, TBMs display a wide range of $CO_2$ source-sink dynamics in the ABZ (Fisher et al., 2014; Huntzinger et al., 2013) and biases compared to observations (Schwalm et al., 2010; Schaefer et al., 2012). Given the criticality of the ABZ to future global carbon balance and the heterogeneity of landscape responses to warming, it is a high priority to understand and address the current biases in TBM carbon cycling.

The Community Land Model version 5.0 (CLM5.0) is the land component of the Community Earth System Mode version 2.0 (CESM2.0). CLM is one of the most widely-used land surface models and contributes to many global intercomparisons (Zhao and Zeng, 2014; Peng et al., 2015; Ito et al., 2016) and future climate projections relevant for scientists and policymakers (Piao et al., 2013, eg, IPCC). The current state-of-the-art release of the Community Land Model (Lawrence et al., 2019, CLM) incorporates several improvements to climatic fluxes and biogeochemistry relevant for the ABZ. A general improvement was observed globally for CLM5.0 compared to past versions of the model (i.e. CLM 4.0 and 4.5). However, a high bias in photosynthesis or gross primary productivity (GPP) at high latitudes remains a well-documented issue (Wieder et al., 2019) in CLM5.0. Thus, we explore the simulation of GPP along with the net ecosystem exchange (NEE) and terrestrial ecosystem respiration (TER) in order to identify biases in simulation of the seasonal carbon balance.

This study assesses the ability of CLM5.0 to accurately represent $CO_2$ fluxes with gridded model simulations, identifies deficiencies in the simulation of ABZ carbon fluxes, and provides a Model Recommendation for application in the ABZ. We provide a step-by-step diagnosis of the major factors contributing to biases in the simulation of the seasonal cycle of $CO_2$ fluxes in CLM5.0. We use FLUXCOM (Jung et al., 2017, 2019, a gridded product based on machine learning), the International Land Model Benchmarking Project (Collier et al., 2018, ILAMB) to assess model results, and in situ data from FluxNet (https://fluxnet.fluxdata.org) and Ameriflux (https://ameriflux.lbl.gov/). We focus our development on the simulation of $CO_2$ fluxes for each ABZ vegetation type in CLM5.0, representing the tundra and boreal forest. We use point-based simulations at eddy covariance (i.e., EC or flux) tower sites to inform the failure or success of each model development test of the phenology and photosynthesis modules in CLM5.0. We validate model development using gridded products and additional flux towers (withheld from the initial model development) before making our final Model Recommendation. As a result, we identify and resolve many of the known biases in the representation of phenology (Richardson et al., 2012), photosynthesis (Lawrence et al., 2019), and carbon allocation in CLM5.0, allowing a more realistic representation of carbon cycling in this rapidly changing ecosystem.

https://doi.org/10.5194/gmd-2020-365
Preprint. Discussion started: 14 December 2020

## 2 Methods

We investigate the seasonal cycle of ABZ $CO_2$ fluxes with CLM5.0 due to its widespread use and significant model improvements from the previous version. These updated processes include snow physics related to snow age and density, canopy snow interactions, active layer depth, groundwater movement, soil hydrology and biogeochemistry, and river transport (Li et al., 2013). Moving away from globally-constant values of plant traits that are challenging to measure, carbon and nitrogen cycle representations now use prognostic leaf photosynthesis traits (Ali et al., 2016, the maximum rate of electron transport or $J_{max}$ and the maximum rate of carboxylation or $V_{cmax}$), carbon costs for nitrogen uptake, leaf nitrogen optimization, and flexible leaf stoichiometry. Stomatal physiology were updated with the Medlyn conductance model, replacing the Ball-Berry (Medlyn et al., 2011). Additionally plant hydraulics have undergone recent improvement in more realistic stress representation (Kennedy et al., 2019). One primary goal with these improvements was to allow for more physically-based parameters that could be informed by observational ecological data, ultimately allowing for better fidelity with hydrological and ecological processes. Land cover inputs to CLM5.0 were updated to capture transient land use changes from the satellite record.

### 2.1 Pan-Arctic CLM5.0 Simulation

We run CLM5.0 at 0.5° by 0.5° grid resolution with meteorology inputs (rainfall, snowfall, 2m air temperature, 2m specific humidity, surface pressure, downward shortwave radiation, downward longwave radiation, 10m wind speed, and cloud cover fraction) from the Global Soil Wetness Project (GSWP3v1,http://hydro.iis.u-tokyo.ac.jp/GSWP3/ ), which is a standard forcing dataset in the Land Surface, Snow and Soil Moisture Model Intercomparison Project (Van den Hurk et al., 2016, LS3MIP). GSWP3v1 has been shown to be appropriate and less biased as a forcing dataset for CLM5.0 simulations in the ABZ (Lawrence et al., 2019, CLM). We begin a simulation of the CLM5.0 release in 1850 and run through 2014 including default time series inputs of $CO_2$, aerosol deposition, nitrogen deposition, and land use change (Lamarque et al., 2010; Lawrence et al., 2016), which are available on NCAR's Cheyenne system (Computational and Laboratory, 2017). We implement a regional simulation of CLM5.0 north of 40° N across both hemispheres, allowing us to focus exclusively on ABZ processes. We confirm the improvements made to the newly updated CLM version 5.0 (Lawrence et al., 2019) through a comparison of CLM version 4.5 with the same input datasets.

For our control CLM5.0 simulation, we use an available equilibrated 1850 intialization on NCAR's Cheyenne system (Computational and Laboratory, 2017) with spun-up carbon pools. After model development, we again spin the model using this initial dataset, and we find GPP to equilibrate quickly, within 20 years (Supplement Fig. S1). To be conservative, we spin-up the model with our recommended model development versions for 100 years to ensure carbon fluxes have come to equilibrium. Then we use this equilibrated state as initial conditions in a production run simulation beginning in 1850 with all the same configuration and climatology as the CLM5.0 release control simulation.

Typical of land surface models, CLM5.0 represents vegetation through broad plant functional types (PFTs). CLM5.0 represents ABZ vegetation using five PFTs: needleleaf evergreen boreal trees (NETs), needleleaf deciduous boreal trees (NDTs), broadleaf deciduous boreal trees (BDTs), deciduous boreal shrubs (hereafter "shrubs"), and arctic C3 grasses (hereafter "grasses"). We focus model development on PFT-specific comparisons, which allows a direct comparison with observational data. Any improvements to PFT specific carbon flux simulations have implications for changing vegetation distributions in the ABZ.

### 2.2 Model Benchmarking and Validation

Benchmarking is the process of quantifying model performance based on observational data considered to be the expected value or truth. We use FLUXCOM (Tramontana et al., 2016; Jung et al., 2017, 2019) to benchmark gridded $CO_2$ fluxes (i.e., gross primary productivity, terrestrial ecosystem respiration, and net ecosystem exchange, or GPP, TER, and NEE) in CLM5.0. FLUXCOM is an upscaled machine learning product based on FLUXNET eddy covariance towers. As a global product, FLUXCOM is particularly useful for filling spatial gaps in tower observations, especially in the relatively data-sparse ABZ. Derived from global MODIS-based vegetation layers Sulla-Menashe and Friedl (2019), FLUXCOM also generates PFT-specific output. Although there are inconsistencies between the PFT classifications, such as the representation of "mixed forests" in FLUXCOM, this allows direct comparisons of the PFT-specific fluxes represented by CLM5.0.

For an independent set of comparisons that includes additional environmental variables, we also use the International Land Model Benchmarking System (Collier et al., 2018, ILAMB). ILAMB is an open-source land model evaluation system that provides a uniform approach to benchmarking and scoring model fidelity. We use ILAMB to benchmark fluxes of $CO_2$, moisture, and heat, in addition to several land surface properties essential for climate responses and feedbacks such as albedo and leaf area index (LAI). Although the focus of our model development is on GPP, TER and NEE tend to respond strongly to changes in productivity (Chapin et al., 2006; Schaefer et al., 2012; Chen et al., 2015). We benchmark these additional interdependent properties in ILAMB to ensure our development generates systematic improvements.

### 2.3 Point Simulation Protocol

Although FLUXCOM is an invaluable tool to fill spatial and temporal gaps in tower observations across the ABZ, it is by definition not as accurate as direct *in situ* observations of $CO_2$ fluxes, for instance measurements from EC towers, which also include helpful ancillary information such as detailed vegetation composition. After benchmarking the aggregated grid cell fluxes, we assess model performance at specific EC towers that measure year-round seasonal $CO_2$ fluxes, which is a standard model development procedure (Stöckli et al., 2008). We aggregate fluxes of $CO_2$ to monthly means from flux towers in the ABZ that are part of the FluxNet (https://fluxnet.fluxdata.org) and Ameriflux (https://ameriflux.lbl.gov/) networks. We screen the tower records to determine if the PFT type in CLM5.0 corresponds to the vegetation described by tower metadata. We choose towers and grid cells with at least three years of sample data before 2014, as that is the end data of GSWP forcing data for CLM5.0. Collectively, the chosen towers that conform to our data requirements span all PFT types over the ABZ (Supplement Table S1). To mediate the sparsity of data, we divide our observational data further into model development sites vs. validation sites. Our chosen model development sites are US-EML (Belshe et al., 2012), CA-QC2 (Margolis, 2018), CA-OAS (Black, 2016, BDT), and RU-SKP (Maximov, 2016), which encompass all of the CLM5.0 PFTs. We verify our work using additional flux tower measurements from FI-SOD (Aurela et al., 2016), RU-Tks (Aurela, 2016), CA-Sf1 (Amiro,

https://doi.org/10.5194/gmd-2020-365
Preprint. Discussion started: 14 December 2020

2016), US-Atq (Oechel et al., 2014), RU-Sam (Kutzbach et al., 2002-2014; Holl et al., 2019; Runkle et al., 2013), and CA-Gro (McCaughey, 2016).

During our model development process, we examine phenology and photosynthesis schemes in CLM5.0 by running point simulations starting in 1901 using the same inputs as our gridded simulations. Points simulations allow for rapid deployment of model tests, while also conserving compute resources. This speed of computation is invaluable for our multiple model development trajectories. We find that for our focus on phenology and photosynthesis, carbon fluxes equilibrate rapidly and a 20-year spin up is sufficient for point simulations (Supplement Fig. S1). We run the point simulations through 2014 and compared the years measured by flux towers with the same years simulated by CLM5.0. We acknowledge that the climatology experienced by a given flux tower and the reanalysis data used as a model input the model are different. Thus, we focus on the mean seasonal behavior of the flux towers and CLM5.0 to guide model development and allow the yearly variance to serve as an uncertainty range for our characterization of flux tower behavior. Additionally, using the mean monthly $CO_2$ fluxes as calibration data can prevent over-fitting of CLM5.0 parameters. Each model development simulation for a specific PFT is also run for the other PFTs at the development sites (CA-QC2, CA-OAS, US-EML, and RU-SKP). After finalizing a given model development scheme, we implement the updates at the withheld EC sites (Supplement Table S1) and in a gridded fashion across our ABZ regional domain.

## 2.4 Model Development

We identify several issues in the phenology and photosynthesis schemes in CLM5.0 for the ABZ, which are detailed in Section 3.1. These can be categorized by (i) extrapolation of schemes and parameterizations designed for temperate vegetation, (ii) biases in the prediction of leaf photosynthetic traits and (iii) mis-specified carbon allocation parameters.

### 2.4.1 Phenology Onset

The representation of spring and autumn phenology for deciduous trees, shrubs and grasses in CLM5.0 is based on a study of the conterminous United States (White et al., 1997) and extended to the ABZ. In the extratropics, plants initiate their photosynthetic growing season in response to various climatic factors in spring, reach peak productivity in summer, and enter dormancy in autumn. This is parameterized in CLM5.0 by allowing spring onset to begin once a threshold for cumulative growing degree days is met, as determined by White et al. (1997) using relationships between temperatures and the satellite based Normalized Difference Vegetation Index (NDVI). Thus, in CLM5.0, onset is based on relationships derived from temperate latitudes and extrapolated to the ABZ. We find that this parameterization requires relatively warm temperatures for the ABZ before onset can begin, which causes a delay in the beginning of the growing season for deciduous plants.

To implement a more mechanistic approach to onset in the ABZ, we identify environmental thresholds that correspond to physiological changes during spring onset in high latitudes. Field observations consistently demonstrate that productivity initiation in the ABZ is governed by the cessation of freezing temperatures and the availability of soil water(Goulden et al., 1998). We use daily output from FLUXCOM and flux towers to identify the initiation of GPP in spring. We then compare the timing of productivity to a variety of CLM5.0 environmental variables known to correspond strongly with GPP onset

(Chapin III and Shaver, 1996; Starr and Oberbauer, 2003; Borner et al., 2008), including soil temperature, soil moisture, soil ice content, air temperature, liquid and ice precipitation, snow depth, and latent and sensible heat fluxes (Supplement Fig. S2). We find that soil temperature (and thus soil ice content in the third soil layer with ~10 cm depth), minimum 2m temperature, and snow cover undergo notable state transitions around the timing of GPP onset, enabling their use as a phenology threshold in CLM5.0.

For our phenology algorithm, we therefore allow photosynthesis to begin when the following environmental criteria occur:

1. the 10-day average soil temperature in the 3rd soil layer is above 0° C
2. the 5-day average minimum daily 2m temperature average is above 0° C
3. when only a thin layer of snow remains on the ground ($< 10$ cm).

Together, these metrics approximate when plants begin photosynthesis in spring, allowing for roots to uptake moisture in unfrozen soil, for air temperatures to be consistently above freezing, and for plants to no longer be covered in snow.

### 2.4.2 Phenology Offset

Fall phenology in CLM5.0 is based on the same study focused on the temperate latitudes (White et al., 1997). As with phenology onset, biases arise from the extrapolation of temperate zone relationships to the high latitudes. Using NDVI, senescence was identified to occur in autumn when daylight decreases ~11 hours. This daylight threshold is then set to be a global constant in CLM5.0. Complete dormancy is reached after 30 days after this photoperiod threshold. In the ABZ, this threshold of 11 hours of total daylight generally causes plants to decrease productivity in October and to begin dormancy in November. In reality, vegetation should be reaching dormancy at the end of September in the high Arctic (Zhang et al., 2004), with senescence beginning in August (Corradi et al., 2005). Based on existing physiological studies of ABZ vegetation, it is unclear if temperature or photoperiod are the driving factor that triggers fall senescence (Marchand et al., 2004; Eitel et al., 2019), or if a combination of both is necessary for ABZ senescence (Oberbauer et al., 2013). Therefore, we focus on photoperiod, which is seasonally more consistent across the ABZ and clearly crucial for photosynthesis. Based on observations at high latitudes, 15 hours is a more accurate timing for senescence above 65° N (Corradi et al., 2005; Eitel et al., 2019). We scale the photoperiod threshold linearly along a latitudinal gradient from 65° N until ~11 hours at 45° N such that the temperate latitudes retain the offset timing determined by White et al. (1997).

### 2.4.3 Day Length Scaling for Photosynthetic Parameters

The Farquhar model of photosynthesis for C3 plants uses two main parameters to represent photosynthetic capacity, $J_{max}$ (the maximum rate of photosynthetic electron transport) and $V_{cmax}$ (the maximum rate of Rubisco carboxylase activtiy). In the current release of CLM5.0, $J_{max}$ and $V_{cmax}$ are predicted by a mechanistic model of Leaf Utilization of Nitrogen for Assimilation (Ali et al., 2016, LUNA). Unlike previous versions of CLM, both $J_{max}$ and $V_{cmax}$ are prognostic in CLM 5.0, which allows for the vegetation to adjust to nutrients and environmental conditions. In our comparison of productivity in

CLM5.0, we find that the prediction of J$_{max}$ and V$_{cmax}$ may be biased high in the ABZ (Rogers et al., 2017) when using algorithm values and schemes more appropriate for the tropics and temperate regions, which contributes to the overestimation of GPP by CLM5.0 across the ABZ.

Currently, J$_{max}$ is scaled in LUNA using day length:

$$f(daylength) = (\frac{daylength}{12})^2 \tag{1}$$

The function, $f(daylegth)$, is a scaling factor that is based on the formulation in Bauerle et al. (2012), which quantifies the relationship between day length and J$_{max}$. However, the denominator in this equation in CLM5.0 is set to 12 hours, when it should be the maximum day length possible at a particular latitude (Bauerle et al., 2012). While 12 hours is fairly representative for lower latitudes, this scale factor does not work for the ABZ where some regions experience up to 24 hour day light in summer, which allows f(daylength) $> 1$ in Equation 1, particularly around the summer solstice in June. To address this, we replace the default denominator of 12 hours with the geographically specific annual maximum hours of daylight that occur for a given grid cell.

### 2.4.4 Temperature Acclimation

Within both the Photosynthesis and LUNA schemes in CLM5.0, J$_{max}$ and V$_{cmax}$ are scaled from their values on the environmental leaf temperature and to 25° C using a modified Arrhenius temperature response function from (Kattge and Knorr, 2007, Supplement Fig. S3). Currently, J$_{max}$ and V$_{cmax}$ are allowed to acclimate to the plant's growth temperature, defined as the 10-day average 2-m temperature. However, the temperature acclimation function is limited to temperatures between between 11° C and 35° C and tuned to mostly temperate species (Kattge and Knorr, 2007). At temperatures outside of the acclimation range, the temperature acclimation function scales J$_{max}$ and V$_{cmax}$ to unusually high values (Supplement Fig. S3), likely due to the use of temperate species for parameterization tuning. The mean daily summer temperature in the ABZ above 60° N is below 11° C (Kalnay et al., 1996, NCEP/NCAR reanalysi)s), which implies vegetation at this latitude may never enter the range for temperature acclimation designated by Kattge and Knorr (2007). The temperature scaling done below 11° C is not based on any ABZ studies, nor does it match the previous scaling used in CLM5.0 parameterizations from Leuning (2002), which do contain some field sites in the ABZ. At more southern locations in the ABZ, vegetation may fluctuate around this minimum threshold value of 11° C, allowing discontinuities to appear in the temperature scaling of J$_{max}$ and V$_{cmax}$ and influencing biases in the seasonality of $CO_2$ fluxes. Due the lack of observational data across the ABZ incorporated in the Arrhenius function for acclimation in Kattge and Knorr (2007) we choose to implement temperature scaling functions from Leuning (2002), which does not create a discontinuity in J$_{max}$ and V$_{cmax}$ at such a critical temperature for the ABZ. This is a standard implementation of the Arrhenius temperature response function, which has been shown to work well at lower temperatures under present climate conditions in previous versions of CLM.

### 2.4.5 J$_{max}$ and V$_{cmax}$ Winter Default

The LUNA module calculates J$_{max}$ and V$_{cmax}$ dynamically during the growing season only. When plants are dormant in winter (non-growing season), CLM5.0 uses constant values.

$$J_{max,t} = \begin{cases} 50, & \text{during winter} \\ J_{max,t-1} + \min[mxcon, J_{max,opt} - J_{max,t-1}] \times J_{max,opt}, & \text{in growing season, if } J_{max,opt} \geq J_{max,t-1} \\ J_{max,t-1} + \max[-mxcon, J_{cmax,opt} - J_{max,t-1}] \times J_{max,opt}, & \text{in growing season, if } J_{max,opt} < J_{max,t-1} \end{cases} \tag{2}$$

$$V_{cmax,t} = \begin{cases} 85, & \text{during winter} \\ V_{cmax,t-1} + \min[mxcon, V_{cmax,opt} - V_{cmax,t-1}] \times V_{cmax,opt}, & \text{in growing season, if } V_{cmax,opt} \geq V_{cmax,t-1} \\ V_{cmax,t-1} + \max[-mxcon, V_{cmax,opt} - V_{cmax,t-1}] \times V_{cmax,opt}, & \text{in growing season, if } V_{cmax,opt} < V_{cmax,t-1} \end{cases} \tag{3}$$

J$_{max,opt}$ (V$_{cmax,opt}$) is predicted by LUNA as the optimal J$_{max}$(V$_{cmax,opt}$) for the plant, which as the name states is optimal and does not account for limitations on enzyme resources. The maximum change constraint ($mxcon$) limits the amount of change for J$_{max}$ (and V$_{cmax}$) based on the resources available to that plant, which can change every time step. This scheme allows J$_{max}$ and V$_{cmax}$ and thus photosynthesis to be co-limited by resources. We find the change constraint to be a reasonable one to place on J$_{max}$ and V$_{cmax}$, as it allows for the climatic history on the grid cell to influence the future prediction of leaf photosynthetic traits. However, this scheme for J$_{max}$ and V$_{cmax}$ is only active during the growing season. In winter when LAI=0 and plants are dormant, J$_{max}$ and V$_{cmax}$ are not predicted by LUNA and instead are given a default global place holder value. Thus, at the start of the growing season (or first day of spring), J$_{max,t}$ and V$_{cmax,t}$ are directly calculated from the last day of winter:

$$J_{max,\text{last day of winter}} = J_{max,t-1} = 50 \tag{4}$$

$$V_{cmax,\text{last day of winter}} = V_{cmax,t-1} = 85 \tag{5}$$

We find that this global default winter value strongly influences the prediction of J$_{max}$ and V$_{cmax}$ throughout the entire growing season (Supplement Fig. S4). In all of the ABZ PFTs, raising these default values increases mean growing season GPP, whereas decreasing them lowers GPP (Supplement Fig. S4). Furthermore, the constant winter values in Equation 3 represent a high bias globally in V$_{cmax}$ (Lawrence et al., 2019), contributing additional bias. Due to the sensitivity of this choice and in an effort to leverage the physiological history of a given location, we choose to save the average predictions of J$_{max}$ and V$_{cmax}$ from the previous growing season for all PFTs (J$_{max,prevyr}$ and V$_{cmax,prevyr}$). We use these pft specific values to initialize J$_{max}$ and V$_{cmax}$, such that on the first day of the growing season,

$$J_{max,pft,\text{last day of winter}} = J_{max,pft,prevyr} \tag{6}$$

$$V_{cmax,pft,\text{last day of winter}} = V_{cmax,pft,prevyr} \tag{7}$$

Then Equations 2 and 3 continue the calculation $J_{max}$ and $V_{cmax}$ for the rest of the growing season.

### 2.4.6 Carbon Allocation

Finally, we investigate the sensitivities of parameters related to carbon allocation, which are relatively uncertain and strongly influence $CO_2$ fluxes in the ABZ, particularly the stem-to-leaf ratio and the root-to-leaf ratio. In CLM5.0, the parameter defining the root-to-leaf allocation ratio is set at a constant value of 1.5 for all PFTs. This is not an ideal configuration as boreal trees and tundra vegetation are structurally different than other plant types due to the need to cope with colder temperatures, which should be reflected in allocation to their roots, leaves, and other plant components. Even within a PFT, different species have been measured to have drastically different ratios of allocation to roots and leaves (Iversen et al., 2015), but for the purpose of circumpolar simulations, we limit our allocation parameters to the PFT level. Root to leaf ratios have been measured as consistently high for grasses and shrubs, meaning more allocation to roots than leaves (Chapin III, 1980; Iversen et al., 2015). We, therefore, tested a higher root-to-leaf allocation of 2 for shrubs and grasses, which agrees relatively well with observations of tundra vegetation (Buchwal et al., 2013). For boreal trees, below ground allocation in evergreen conifers has been found to be higher than in deciduous trees (Gower et al., 2001; Kajimoto et al., 1999). Lowering the root-to-leaf ratio of DBT better represents the typically shallow root systems of deciduous boreal trees (Kobak et al., 1996), while being consistent with values implemented in other deciduous tree modeling studies (Arora and Boer, 2005, e.g., 0.75). Observations suggest that boreal NETs in general have more extensive root systems than the deciduous trees (Gower et al., 1997), thereby requiring more belowground resources, and that tundra shrubs and grasses allocate even more photosynthate belowground. Thus, observations provide support for NET root-to-leaf allocation to be larger than DBT, and we choose to allow the NET root-to-leaf allocation to remain at the CLM5.0 default value.

Regarding stem allocation, CLM5.0 includes an option for dynamic stem-to-leaf allocation. The ratio is based on NPP and can be used for woody trees and shrubs (Friedlingstein et al., 1999), generally acting to increases woody growth in favorable conditions (Vanninen and Mäkelä, 2005). Though this allocation was previously used in CLM4.5 and turned off for CLM5.0, it is an uncertain choice as noted explicitly in Lawrence et al. (2019). A problem with this allocation scheme was noted in the tropics (Negrón-Juárez et al., 2015), but not in temperate or high latitude climates. We test both options, comparing the static stem-to-leaf ratios used in CLM5.0 to the dynamic allocation option.

## 3 Results

We investigate the simulation of $CO_2$ fluxes in the arctic-boreal zone by CLM5.0 using gridded and point simulations. We identify biases in the carbon cycle in Section 3.1, present our mechanistic and additive improvements to phenology and photosynthesis in Section 3.2, and make our model recommendation in Section 3.3. This ABZ analysis focuses primarily on GPP fluxes in CLM5.0, but as expected, our assessment extends to TER and NEE due to the interdependence of these carbon fluxes on productivity (Chen et al., 2015). We assess simulation biases based on the comparison of CLM5.0 output against FLUXCOM and EC towers, as detailed in Section 2.2. We address the biases that arise from using the default CLM5.0 parameters and

https://doi.org/10.5194/gmd-2020-365
Preprint. Discussion started: 14 December 2020

schemes described in Section 2.4, which can be classified as: (1) phenology onset, (2) phenology offset, (3) daylight scaling, (4) Leuning temperature scaling, (5) initial spring value of $J_{max}/V_{cmax}$, (6) dynamic stem-to-leaf carbon allocation, (7) realist root-to-leaf carbon allocation.

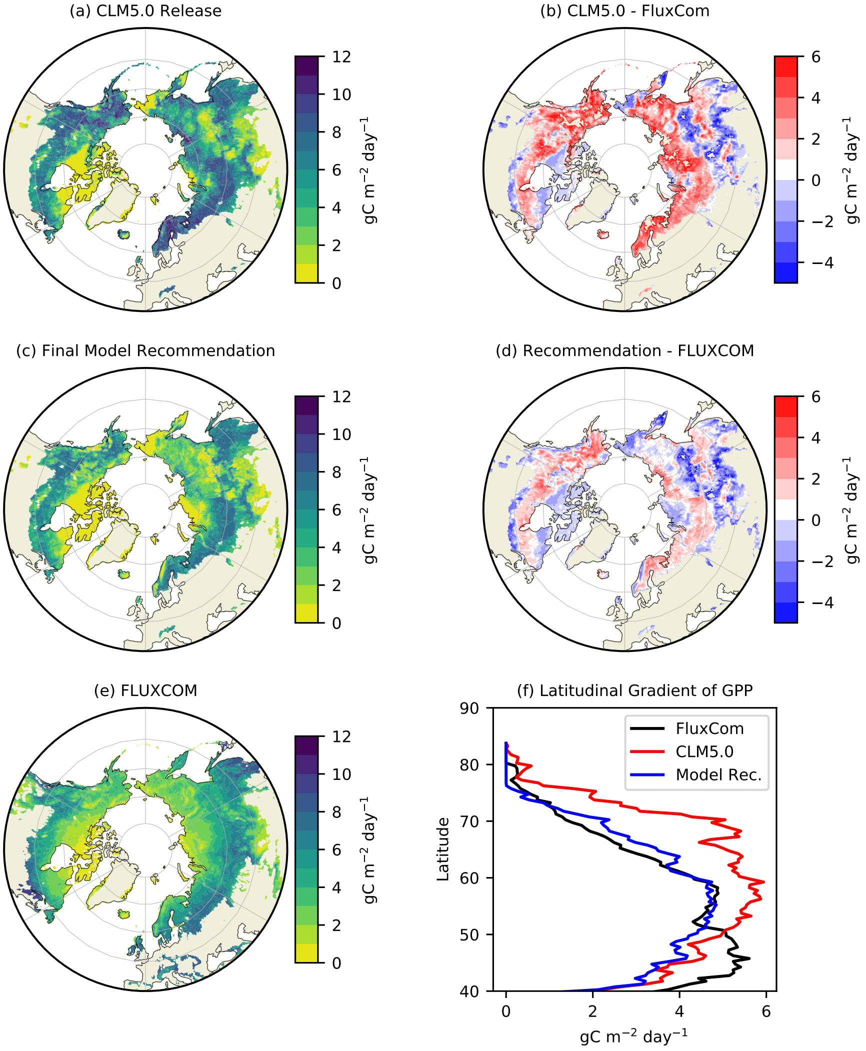

**Figure 1.** Average Summer (JJA) GPP (gC $m^{-2}$ day $^{-1}$) for (a) CLM5.0 Release, (b) our Model Recommendation, and (c) FLUXCOM, with the difference between model simulation and FLUXCOM in (b) and (d). The latitudinal gradient of summer GPP is depicted in (f).

## 3.1 Biases in CLM5.0

The latest release of CLM5.0 substantially overestimates summer GPP in the ABZ by $\sim$3 gC m$^{-2}$ day$^{-1}$ or 40% (red line in Figures 1b and 2a). The magnitude of this bias is such that CLM5.0 estimates of GPP for high latitudes tundra vegetation are comparable with the more southern boreal forests (Fig. 1a). This lack of a latitudinal gradient in CLM5.0 is not supported by FLUXCOM and ILAMB benchmarking (Fig. 1f). Though most of the ABZ in CLM5.0 is over productive, we note that there is a large area with $GPP = 0$ in Siberia, indicating that this region is not photosynthesizing in CLM5.0 though it should be. Thus, the simulation of carbon fluxes in CLM5.0 is very heterogeneous with areas that are highly productive and areas that are not-functioning, or "dead-zones".

We next investigate the seasonal cycle of $CO_2$ fluxes in the ABZ. Across the ABZ, average productivity in the CLM5.0 simulation is high throughout the year compared to FLUXCOM, which is shown throughout the year in Figure 2a. From a seasonal perspective, CLM5.0 vegetation enters dormancy later than observations, as can be seen by the high biases in GPP in fall. The timing of photosynthesis in spring does, however, appear accurate when we look at the PFT-aggregated average of $CO_2$ fluxes. We see a similar high bias in TER in Figure 2b, as respiration is tightly coupled to the high biased GPP. The magnitude of peak summer NEE in CLM5.0 matches observational data better than GPP and TER. However, its seasonal cycle exhibits biases and timing issues related to spring drawdown, summer minimum, and fall peak NEE (Fir. 2c).

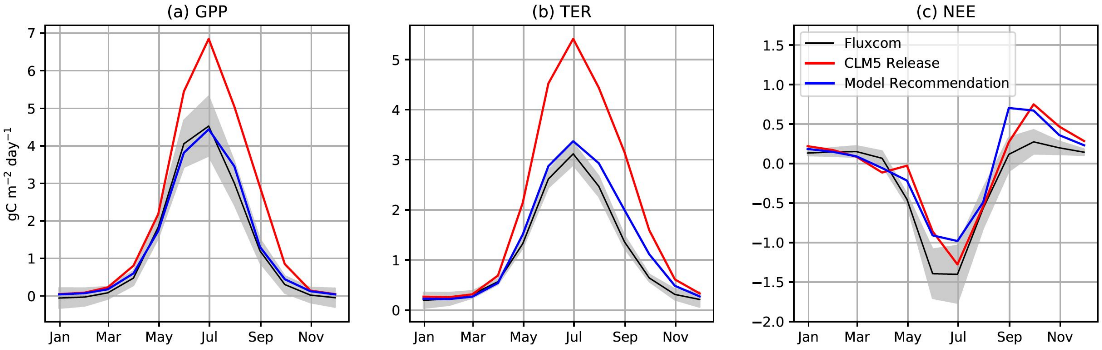

**Figure 2.** The annual cycle of (a) GPP, (b) TER, and (c) NEE from CLM5.0 and our Model Recommendation compared to FLUXCOM in the ABZ. Non-productive grid cells in the ABZ are removed from the average, meaning where LAI=0, which is standard procedure in CLM analysis (Lawrence et al., 2019).

Assessing the seasonality of $CO_2$ fluxes in the ABZ using the PFT-specific output of CLM5.0 reveals biases in phenology that are hidden when PFTs are aggregated together in a grid cell. In terms of phenology, we find that NET begins significant photosynthesis in February in CLM5.0 when air temperatures are well below freezing. This onset of NET photosynthesis is considerably early according to both FLUXCOM (Figure 3b) and our understanding of available liquid water for photosynthesis (Goulden et al., 1998). The peak productivity in NET occurs in June, instead of July as seen in observational data. In contrast, the onset of photosynthesis for deciduous trees and shrubs is consistently late (Fig. 3). The gridded CLM5.0 GPP output hides these biases, showing that on average onset in CLM5.0 matches observations (Fig. 1a). In contrast, the high bias of CLM5.0 productivity during late autumn was easily seen in the gridded CLM5.0 output, and we confirm that this bias is due to the shifted seasonal cycle of deciduous PFTs (Fig. 3).

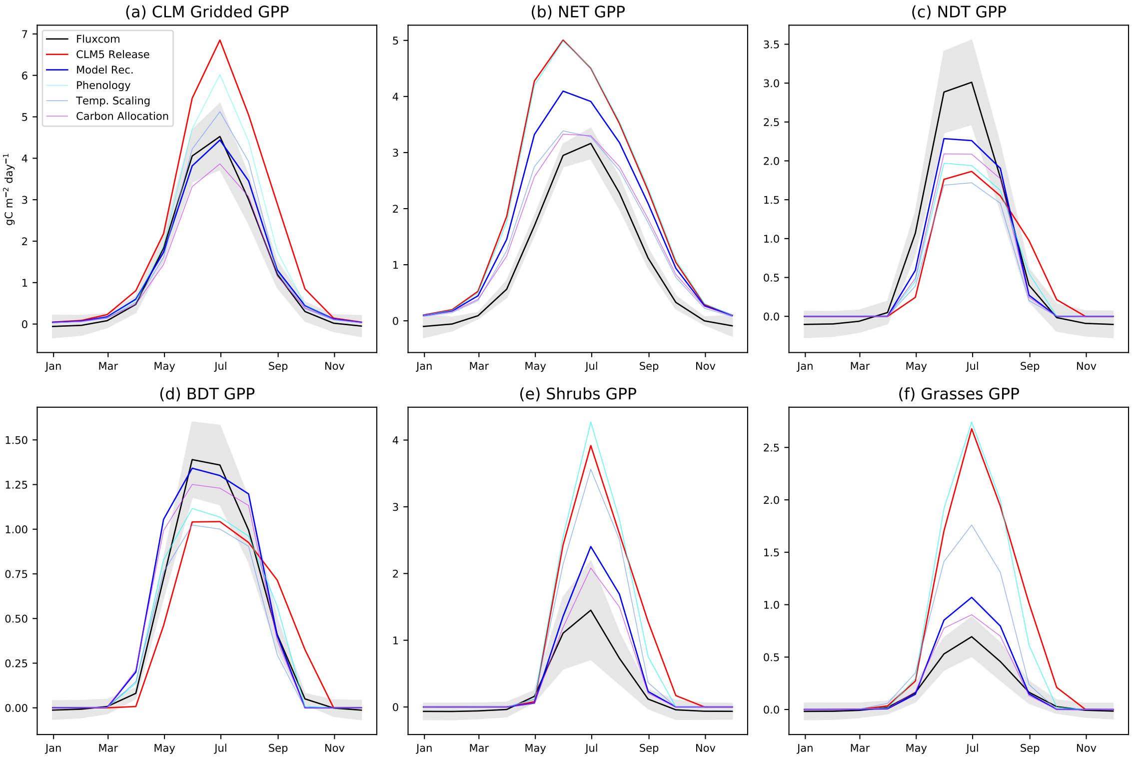

**Figure 3.** The annual cycle of GPP for CLM5.0 release with intermediate model development steps compared to FLUXCOM for: (a) aggregated gridded CLM5.0 output, (b) NET, (c) NDT, (d) BDT, (e) shrubs, (f) grasses. Phenology incorporates changes to onset/offset. Temp. Scaling adds our scaling of J$_{max}$ and V$_{cmax}$ by daylight and Leuning. Carbon allocation adds changes to the root-to-leaf and stem-to-leaf parameters. The final model recommendation incorporates the bug fix (Supplement Section 3) and spring initialization of J$_{max}$ and V$_{cmax}$.

Regarding the magnitude of photosynthesis, the CLM5.0 PFT-specific output indicates that both shrubs and grasses have a large high bias of GPP compared to observational data by a factor of 2-3 (Fig. 3a). We confirm that the tundra grass and shrub PFT specific output is often greater than or as productive as the boreal trees in CLM5.0 (Fig. 3 e,f vs. b,c,d). The deciduous boreal trees (NDT and BDT) have a low growing season GPP bias, while NET have a high productivity bias. By examining the spatial pattern of the average summer GPP (Fig. 1), one can see that there are many areas where $GPP = 0$ for many consecutive years, indicating that the PFT did not survive. In Siberia, a prominent "dead zone" occurs in what should be highly productive deciduous needleleaf larch forests. Smaller "dead zone" areas are present for all other PFTs across the ABZ (Supplement Fig. S5).

As with the aggregated CLM5.0 output, the PFT specific biases in TER are similar to those noted for GPP (Supplement Fig. S6). PFT-specific patterns in NEE also tend to follow the biases in GPP and TER, with the notable exception of spring in deciduous vegetation. For these PFTs, there is a large spike of $CO_2$ release to the atmosphere, up to 0.5 gC $m^{-2}$ $day^{-1}$ between April and May that does not match observations (Supplement Fig. S7). This is primarily due to the late onset photosynthesis at a time when TER is increasing due to warming air and soil temperatures. We that the net balance of BDTs is near 0, rather than a sink, which agrees with our conclusions that deciduous trees are not productive enough relative to FLUXCOM and flux towers. Ultimately, the timing and magnitude of biases in TER and NEE confirm our need to focus on GPP at a first step in better representing seasonal CO2 fluxes in CLM5.0 for the ABZ.

Benchmarking CLM5.0, yields the following primary issues for the simulation of GPP across the ABZ:

1. The onset of GPP in deciduous PFTs in spring is consistently late across all PFTs.
2. The fall senescence of GPP is consistently late.
3. There is no latitudinal gradient in summer GPP, due in part to the high GPP bias in tundra grasses and shrubs.
4. NET begin photosynthesis early in winter and reach peak in productivity in June, instead of July.
5. NET have a high GPP bias throughout the growing season.
6. Deciduous trees (BDT and NDT) have a low GPP bias.
7. There are large areas of PFTs that have no productivity at all or are effectively dead in CLM5.0, particularly the NDT in Siberiak, representing larch forests (larix spp.).

### 3.2 Model Development at Flux Towers

We confirm these biases in the ABZ by comparing the CLM5.0 PFT-specific output to representative flux towers across the ABZ. For example, the southern boreal mixed forest site at CA-QC2 (Figure 4a) contains NET, BDT, and shrub PFTs. The BDT here is a dead zone, where $GPP = 0$, making it a useful site to understand what model thresholds may be influencing one PFT to die out in a simulation, while others remain productive. We also include a BDT site at CA-OAS (Figure 4b) to further investigate the simulation of deciduous trees at an alive grid cell in CLM5.0. The grasses and shrubs at Eight Mile Lake, Alaska are approximately five times more productive than observations (Figure 4c). In contrast, at the larch forest at RU-SKP (Figure 4d), we find that onset is late and GPP is roughly half the observed value, consistent with the low bias in NDT gridded output. We perform model development by examining each issue described in Section 2.4 sequentially on our model development sites: CA-QC2, CA-OAS, US-EML, and RU-SKP. Each flux tower measurement is carefully chosen to cover all CLM5.0 PFTs to understand their complex impacts on GPP across all PFTs, while also including a "dead-zone" to tease out a different kind of bias. Model development follows the procedure and biases described in Section 2; we begin with phenology, move on to the photosynthesis schemes, and end with adjusting the carbon allocation parameters.

Regarding phenology, high-latitude deciduous vegetation in CLM5.0 initiates photosynthesis too late in the spring. The parameterization from White et al. (1997) did not allow for ABZ vegetation to pass a growing degree day threshold until roughly May or later, as it was developed for temperate ecosystems and extrapolated to the ABZ. We find that using new thermal and moisture thresholds for onset causes the deciduous plants to begin photosynthesis earlier in the season, which more closely matches observations (Fig.3). We also generate a more accurate fall simulation by replacing the 11 hour global offset photoperiod with a latitudinal gradient threshold, ranging from 15 hours to 11 hours. The timing of photosynthesis is critical to understanding changes in the carbon cycle in the ABZ, and we find these mechanistic schemes offer a better ABZ simulation of phenology (Fig.3). However, the bias in the magnitude of photosynthesis is not improved by our phenology changes; In fact, the productivity of grasses and shrubs increases further with a growing season that begins earlier in Spring (Fig. 3e,f, comparing the red "CLM5.0 Release" line to the cyan "Phenology" line).

We test a variety of changes to CLM5.0 photosynthetic schemes and parameters as detailed in Section 2.4. Regarding $J_{max}$, we find that modifying the function that scales $J_{max}$ to accurately use the maximum number of daylight hours on each grid cell (Bauerle et al., 2012) decreases productivity across all PFTs (Figure 4 and Supplement Fig. S8). In particular, we decrease the June spike in GPP for NET because the daylight fraction around the summer solstice is no longer greater than 1. Overall, this modification decreases the high bias in ABZ GPP by 2 gC/m$^2$ in the summer (Supplement Fig. S8) and generates a latitudinal gradient in the PFT specific output of trees (Supplement Fig. S5). By reverting the CLM5.0 temperature scaling scheme from (Kattge and Knorr, 2007) to Leuning (2002) as used on CLM4.5, we find that GPP is decreased for all PFTs, especially in spring when the photosynthesis ramp up had been artificially high. Our model updates improve phenology of NETs due to more realistic scaling of $J_{max}$ and $V_{cmax}$ (Fig. 3b, the light blue "Temp Scaling" simulation). The GPP of grasses is also decreased, but shrubs are still biased high.

After decreasing productivity of all PFTs (Fig. 3, compare the red "CLM5.0 Release" with the blue "Temp. Scaling"), tundra shrub and grass productivity in CLM5.0 retain a substantial high GPP bias (Fig. 3e,f), while the deciduous tree PFTs have a low GPP bias (Fig. 3c,d), which may be related to non-optimized ABZ carbon allocation parameters. Allowing for a dynamic stem-to-leaf allocation improves both the timing and magnitude of photosynthesis (Supplement Fig. S9). Additionally, we make PFT specific alterations to root-to-leaf ratios based on our findings from Section 2.4. As a result, GPP is lowered in grasses and shrubs and increased for deciduous trees (NDT and BDT), approaching FLUXCOM values (Fig. 3). The rest of our changes to the model involve schemes in LUNA that we believe are initialized incorrectly for the ABZ, but also the rest of the world. These recommended model updates include initializing the winter default values of $J_{max}$ and $V_{cmax}$ using the mean value for a given grid cell during the previous growing season (Equations 4,5 and Supplement Fig. S4) and a model error related to the calculation of 10-day leaf temperature (Supplemental Section S3).

### 3.3 Model Recommendation

Based on our changes to phenology, photosynthesis, and carbon allocation schemes, we recommend the following mechanistically based changes to CLM5.0 for a considerably improved representation of CO2 fluxes in the ABZ:

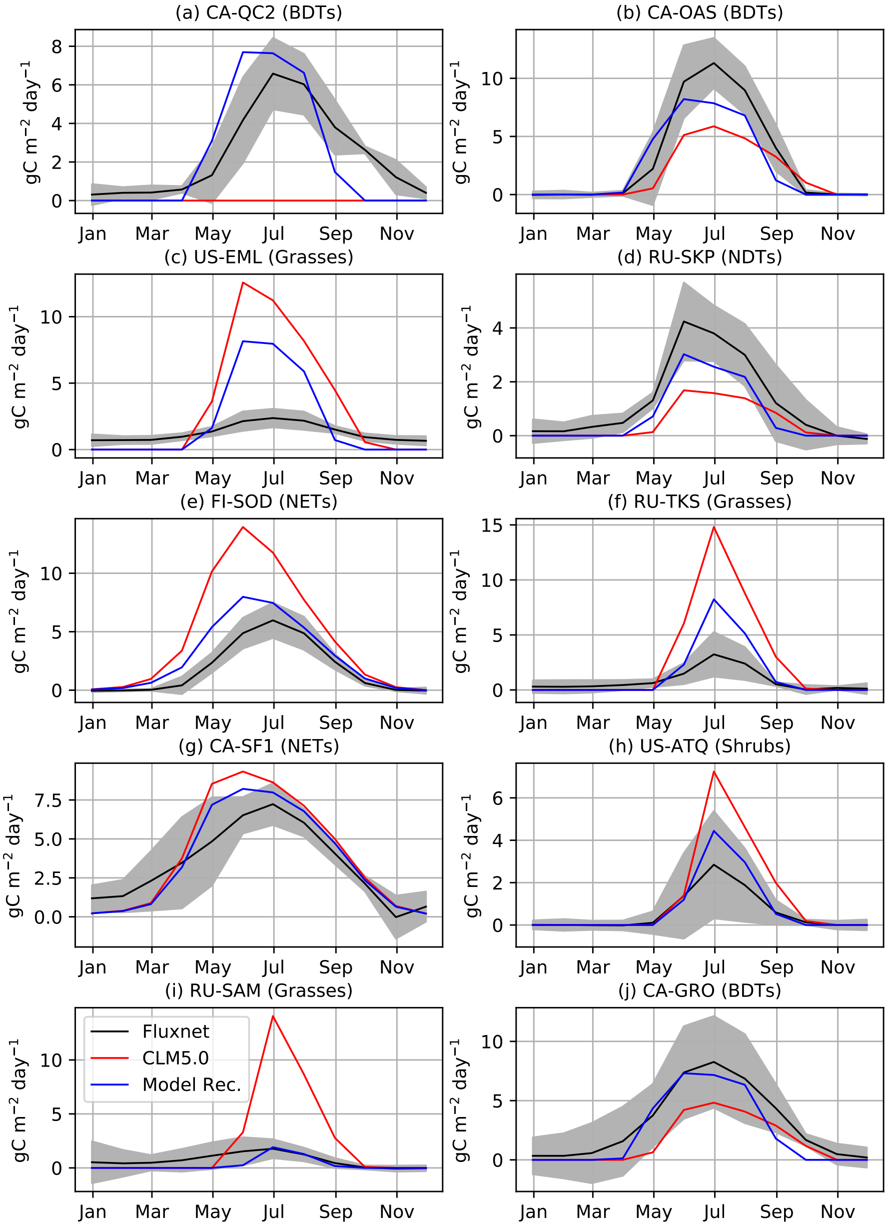

**Figure 4.** Comparison of GPP at Flux Tower sites to the CLM5.0 release and the results of our model development. We performed model development at CA-QC2 (mixed forest site in Quebec), CA-OAS (Aspen forest in Saskatchewan), US-EML (Eight Mile Lake Tundra location), and RU-SKP (Yakutsk Spasskaya Larch Forest). We did additional comparisons with FI-SOD (Sodankyla, Finland), RU-TKS (Tiksi grasslands), CA-SF1 (Saskatchewan boreal forest), RU-COK (Chokurdakh Tundra shrubs), RU-SAM (Samoylov grasslands), and CA-GRO (Groundhog River Boreal Forest).

1. GPP onset is based on soil temperature, air temperature, and snow cover.
2. GPP offset is based on a latitudinal photoperiod gradient such that the high Arctic begins senescence earlier.
3. $J_{max}$ is scaled by maximum day length instead of a constant 12 hours.
4. $J_{max}$ and $V_{cmax}$ are scaled by temperature response functions parameterized by Leuning (2002).
5. $J_{max}$ and $V_{cmax}$ have initial values in spring that are based on the LUNA predictions from the previous growing season, allowing the values to vary across PFTs, time, and space.
6. The stem-to-leaf carbon allocation ratio for trees and shrubs is allowed to be dynamic throughout the season.
7. Observationally based root-to-leaf carbon allocation ratios are used. For deciduous tree PFTs, the root-to-leaf ratio is decreased, while the ratio for shrubs and grasses is increased.

We compare our model improvements in a gridded simulation against $CO_2$ fluxes from FLUXCOM (Figure 2a). The high productivity bias at high latitudes is substantially reduced due to our model development by decreasing the productivity of ABZ shrubs and grasses. Our Model Recommendation for CLM5.0 produces a latitudinal gradient (Fig. 1f) in productivity, with the tundra no longer being as productive as the boreal forest (Fig. 3). The timing of photosynthesis is also improved as dormancy is reached by October in most PFTs, instead of November (Figs. 1 and 3). In examining the PFT specific output (Fig. 3), we confirm an earlier beginning to spring photosynthesis in deciduous trees, shrubs, and grasses. In contrast, our model development successfully delays the onset of productivity in NET, due to a combination of daylight scaling and the temperature scaling from Leuning (2002). As for the magnitude of photosynthesis, we find that NET photosynthesis is reduced across the ABZ, while the deciduous boreal tree PFTs experience an increase in productivity (Supplement Fig. S10).

Our modifications to CLM5.0 offer similar improvements to simulations of $CO_2$ fluxes when looking at specific flux towers (Fig. 4), such as the increase in productivity of BDT at CA-OAS, which is further validated at CA-GRO. Photosynthesis in NDT is increased due to our model development, but as shown in both gridded output and RU-SKP, the NDT photosynthesis needs to increase further. The phenology and magnitude of NET is much improved at validation sites. However, as is expected (Schaefer et al., 2012), not all of the flux tower sites have $CO_2$ fluxes that are reproduced within the range of observational uncertainty (Fig. 4c and Supplement Fig. S11). For example, although GPP at US-EML is reduced due to our model development, it is still biased high. However, the grasses and shrubs at other validation sites are much closer to flux measurements, like the grasses and shrubs at RU-SAM, RU-TKS, and US-ATQ.

Although GPP is our main focus of development, we find improvements in other component $CO_2$ fluxes. Changes in TER generally follow those of GPP, and our modifications substantially reduce the high summer respiration bias in CLM5.0 (Fig. 2), which is mostly due to the reduction of GPP and TER in grasses and shrubs at high latitudes(Supplement Fig. S6). The respiration of deciduous tree PFTs did not change substantially, but TER decreases in NET due to the decrease in GPP. Due to the improvements in GPP onset/offset, the model no longer simulates large net $CO_2$ emissions in spring (Supplement Fig. S7), which better matches observations. However, in many PFTs the respiration in fall is high in the gridded output. Although this does not match FLUXCOM, it is consistent with recent measurements of high fall respiration in the ABZ (Commane et al., 2017; Natali et al., 2019).

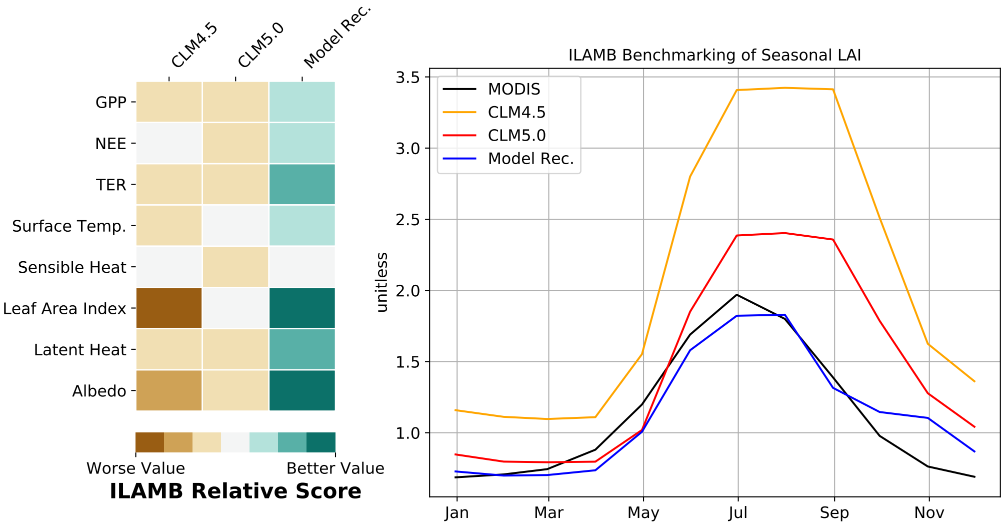

**Figure 5.** ILAMB score of CLM5.0 Model Development Recommendation against previous versions of CLM: 5.0 and 4.5.

Comparing output from CLM5.0 and our Model Recommendation to observational data provided by the ILAMB framework confirms broad improvements in model fidelity (Fig. 5). This includes the $CO_2$ fluxes we focus development on, as well as surface fluxes (sensible heat, latent heat, albedo). ILAMB confirms that the high GPP bias and late phenology biases are reduced. LAI, in particular, has been improved greatly in the Arctic in regards to both timing and magnitude (Fig. 5). According to the ILAMB score, the implemented changes are not detrimental to any other essential land surface variables, and in fact improve their simulation according to the centralized benchmark scores. The relative improvements to moisture and heat fluxes are particularly noteworthy, as these changes can feed back to the regional climate system.

## 4 Discussion

We have approached model development for $CO_2$ cycling in the ABZ in a mechanistic and targeted fashion, leveraging available observational data and derived products. We find that many biases are interconnected, meaning that mechanistic model development and bug fixes can improve part of the simulation, while making other aspects worse (Fig.3). Overall, our work with CLM5.0 in the ABZ highlights the importance of regional model analysis and development. We find the extrapolation of model schemes developed for temperate latitudes to the high latitudes to be the root of many biases, as has also been noted elsewhere (Rogers et al., 2017).

Having more accurate phenology in CLM5.0 is critical for understanding the recent and future changes in biogeochemistry in the ABZ, as global change drivers during the shoulder seasons may be drivers of carbon cycle changes. The growing degree threshold in the CLM5.0 release is not met until late spring for deciduous plants (Figure 3), consistently delaying the spring onset. Using air and soil temperatures combined with snow depth as a metric for spring onset more accurately captures spring productivity timing in deciduous trees, shrubs and grasses across the ABZ (Fig. 4). We find that the freeze-thaw transition simulated by CLM5.0 matches the timing of photosynthesis across vegetation types and latitudes from other studies (Botta et al., 2000; White et al., 2009) as well. Our new metric thresholds account for the key environmental conditions that signal the end of winter, as deciduous trees have protective mechanism to avoid the onset of growth when there is a strong probability of cold snaps (McMILLAN et al., 2008). By combining a snow threshold with our air and soil temperatures metrics, we prevent the more southern boreal forest from beginning photosynthesis too early (model sensitivity tests not pictured). This new onset scheme in our model recommendation also causes some areas with dead PFTs to begin photosynthesizing. The previous growing degree day scheme in CLM5.0 required soil temperatures to sum to a threshold before the summer solstice, meaning cold soil temperatures prevented photosynthesis from ever starting, causing some of the “dead” PFTs in CLM5.0. The deciduous (needleleaf and broadleaf) trees in CLM5.0 become more productive in summer as their growing season is allowed to begin earlier, which is desirable due to their low GPP bias. The grasses and shrubs increase further in productivity after more mechanistic phenology drivers are applied, meaning the previous phenology parameterization is not the cause of their high bias.

We implement an offset scheme with a latitudinal gradient in CLM5.0, where the offset day length decreases linearly from15 hours at 65° N to 11 hours at 45° N. This is a first step towards more realistic timing of fall senescence in CLM5.0, and additional work is needed to understand how temperature and other climate drivers impact the timing of dormancy. Studies are divided on the issue of whether temperature or photoperiod are driving offset in the ABZ. Field experiments have found photoperiod to be a likely driver at high latitudes (Eitel et al., 2019), but temperature and even precipitation may be more important at lower latitudes. Experiments of high arctic tundra have shown that senescence can be delayed by up to 15 days due to warming (Marchand et al., 2004). Given this uncertainty, we suggest that photoperiod is a sufficient and justified approximation for fall dormancy, until better mechanistic relationships can be derived from observational data. The late bias in fall phenology has also been noted in other TBMs (Richardson et al., 2012), also likely due to extrapolation of temperate schemes to the high latitudes. Thus, our simple daylight threshold here could be applicable to other models.

One of the most impactful changes to CLM5.0 GPP is the use of maximum day length to scale $J_{max}$, rather than 12 hours. Equation 1 would previously scale the prediction of $J_{max}$ high, particularly in June with the summer solstice and day length at its maximum. The previous use of 12 hours for maximum day length is likely a holdover from using LUNA in the tropics, as (Bauerle et al., 2012) was the cited basis for Equation 1, which used maximum day length appropriately. After we fix this substantial scaling bias, we find other algorithms and parameterizations are more sensitive to model changes. This opens up many avenues of model development, some of which we are able to accomplish in this study, like more realistic allocation parameters and scaling changes to $J_{max}$ and $V_{cmax}$. For future steps, we argue that a re-parameterization CLM is necessary, as previous model tunings attempted to bring down the high GPP bias through parameter choices rather than this bug fix.

As with the length of day scaling described above, the photosynthetic temperature acclimation in scaling of J$_{max}$ and V$_{cmax}$ were not created for ABZ latitudes and tend to exacerbate model biases. We, therefore, recommend not using these functions, and stress the need for further research on photosynthetic temperature acclimation in the ABZ, especially for projecting responses to future climate. The current implementation generates unrealistic seasonal temperature response functions for GPP resulting in model biases (Smith et al., 2017). The temperature acclimation equations are strictly only valid between 11° and 35° C (Kattge and Knorr, 2007), and below that value, J$_{max}$ and V$_{cmax}$ have a scaling discontinuity that biases GPP (Supplement Fig. S3). Previous work by Rogers et al. (2017) advocated for removing this 11° C, but our tests of this did not decrease productivity of the grasses and shrubs at high latitudes (not shown), at least not without a re-parameterization of the acclimation scheme. Recently, Kumarathunge et al. (2019) have created an acclimation parameterization that included ground measurement sites from Utqiagvik (Barrow), Alaska and Finland. Though most of Canada and Siberia are not represented in the parameterization, including this recent observationally-based acclimation function in CLM5.0 is a logical next step for a better ABZ simulation that includes temperature acclimation, critical for simulating GPP under warming climate conditions.

The initialization of J$_{max}$ and V$_{cmax}$ in spring is a highly sensitive choice (Supplement Fig. S4). We find improvements in GPP when using the mean predicted value of J$_{max}$ and V$_{cmax}$from the previous year as an initial spring value. The default values for spring J$_{max}$ and V$_{cmax}$ in CLM5.0 are high for ABZ PFTs (Lawrence et al., 2019). Now with a default value that considers the PFT and climatological conditions of J$_{max}$ and V$_{cmax}$, the simulated seasonal cycle of J$_{max}$ and V$_{cmax}$ mimic the timing of GPP more closely. We observe only very small temporal fluctuation in these average values of J$_{max}$ and V$_{cmax}$, indicating that the LUNA predictions are relatively stable for each geographic-climatological region. The productivity for most ABZ PFTs is decreased throughout the whole summer due to this change in CLM5.0. Though we note that LUNA simulates lower values of J$_{max}$ and V$_{cmax}$ in most Arctic-boreal PFTs, this implementation of average J$_{max}$ and V$_{cmax}$ allows for spatial and temporal variability, including increases of J$_{max}$ and V$_{cmax}$ in some locations. Therefore, there is potential for this scheme to improve future predictions, as the sensitive initialized spring values can now adjust in a warming climate.

Finally, we examine the carbon allocation parameters in CLM5.0, which are a considerable and long-standing source of uncertainty in TBMs. Franklin et al. (2012) appropriately called carbon allocation the "Achilles' heel of most forest models". We argue that CLM5.0 does not use ideal carbon allocation values for the ABZ, but there are multiple diverging development paths for carbon allocation (Fisher et al., 2019) that could lead to a better simulation. During model development and testing of carbon allocation ratios for roots, leaves, and stems, we attempt to balance static and dynamic allocation schemes, but acknowledge there is always room for further development and improvement. Our results suggest that altering carbon allocation ratios, particularly stem-to-leaf and root-to-leaf, to values more consistent with observations improves CO$_2$ fluxes across the ABZ . The default parameters in CLM5.0 do not utilize dynamic stem-to-leaf carbon allocation due to exponential increases in biomass in the tropics (Negrón-Juárez et al., 2015), but not necessarily for the ABZ. We find that simulations of productivity are improved across all ABZ PFTs when this ratio is dynamic. In the model, the previous year's NPP is used to set this ratio, based on the assumption that NPP can serve as a proxy for environmental conditions that send resources to either roots or leaves, thereby increasing woody allocation in favorable growth environments (Vanninen and Mäkelä, 2005). In the previous version of CLM, CLM4.5, dynamic stem-to-leaf allocation generally lowered carbon allocation, sending more carbon to leaves

https://doi.org/10.5194/gmd-2020-365
Preprint. Discussion started: 14 December 2020

than stems, agreeing with observational comparisons (Montané et al., 2017), which is the same pattern we see in ABZ PFTs in CLM5.0. The final improvements to the deciduous tree PFTs, grasses, and shrubs come from changing the root-to-leaf ratio, which is currently the same constant value for all PFTs. Increasing allocation to roots for the grasses and shrubs was advocated in the CLM5.0 documentation for lower latitudes and field observations agree with this choice for the high latitudes (Iversen et al., 2015). Observations also support decreasing the allocation to roots and increasing allocation to stems for deciduous trees in the ABZ (Gower et al., 2001). Ultimately, these static carbon allocation ratios are our best estimation for emergent plant processes, but a more dynamic scheme may be needed for future model versions. For instance, the carbon allocation to roots may saturate when LAI=1 in Arctic shrubs (Sloan et al., 2013). Allowing TBMs to adjust these carbon ratios based on LAI, may be the next step in CLM5.0 model development, approximating the realistic behavior of plant species.

The “dead zones" in CLM5.0 are caused by a combination of issues. For instance, modified onset and offset formulations allowed for some “dead zones” to become productive in our simulations, due to a previously long growing season using all available resources and/or the onset threshold not being reached before the summer solstice. Other non-productive areas were improved by changing the deciduous tree PFT allocation parameters to send more resources to leaves, agreeing with observations and other models (Arora and Boer, 2005). However, these increases in productivity do not clearly and substantially improved the dead PFTs in CLM5.0, particularly the non-productive area of Siberia (Fig. 1c). These areas of non-productivity are particularly problematic for future CLM5.0 simulations due to the suspected importance of Siberian $CO_2$ fluxes for current and future seasonal carbon balance (Zimov et al., 1996, 1999; Lin et al., 2020). Although we did not cause any additional areas to die, we also did not succeed in increasing productivity in the larch forests of Siberia. It is also worth noting that areas with “dead zones” clearly visible in the gridded product have all PFTs dead, not just NDT. We hypothesize that there may be thresholds for climatic drivers that inhibit photosynthesis. For instance, there is a minimum relative humidity threshold for nitrogen allocation in LUNA. This threshold appears to be somewhat arbitrary and the ABZ often experiences a dry continental climate. The larch forests of Siberia could benefit from a lower relative humidity threshold to raise their low productivity and potentially improve “dead zones”. A test of this hypothesis does raise productivity for deciduous tree PFTs, but the “dead zones” do not become productive. We require more information on relative humidity and nitrogen allocation at low temperatures to determine if this parameter should be changed in the model. Here we focus on mechanistic model development, but a parameter specific to ABZ vegetation may lead to further improvements.

The relative improvements to each PFT are also significant. For instance, as noted previously, our model recommendation generates a latitudinal gradient in CLM5.0 (Fig. 1f), which is due to tundra vegetation being less productive. The Arctic grasses and shrubs are now less productive than the boreal trees, which is consistent with observations. The deciduous tree PFTs in our model recommendation are more productive than the CLM5.0 Release, with NDT productivity increasing by 20% and BDT increasing by 50% (not shown). Additional work is needed for the deciduous schemes, as deciduous trees are observed to be more productive than evergreen trees (McMILLAN et al., 2008). We did decrease the high bias of productivity in NETs by 20%, but NET are still causing a high bias in the simulation of GPP. The evergreen scheme has long been noted to be relatively simple in CLM5.0 (Lawrence et al., 2019) and a key next step for model development.

As with most studies of the high latitudes, we are limited by the availability of ground observations. For instance, we only have one flux tower corresponding to NDT (RU-SKP), which is also unfortunately a PFT in CLM5.0 that needs substantial work, particularly in the "dead-zone" in Siberia (Supplement Fig. S5). For other PFTs we restrict our tower choices to have the best data available. We only include EC flux observations where the vegetation classes corresponded with the CLM5.0 PFTs that occur within the ABZ. Metadata indicating a mixed forest or a combination of short stature vegetation and trees causes comparisons to not be clean (Supplement Fig. S11), meaning we withhold these kind of sites for extra validation, but they are not ideal sites for comparison with CLM5.0. The EC record must also span over at least three consecutive years before 2014 due to the forcing dataset used by CLM ending in 2014, which does not allow us to leverage the most recent ABZ ground observations. These criteria restrict our point-based analysis to only a few sites (Supplement Table S1), which does further limit our ability to make statistically robust conclusions. We attempt to mitigate this lack of data by separating the flux towers into model development sites and validation sites, while also including gridded simulations in the validation of our model development. More comprehensive model improvements for the ABZ may be possible through an increase in the availability and spatial representativeness of tower EC data. We look forward to the increased emphasis on data archiving, standardization, and synthesis, as well as more detailed examination of functional relationships and PFT-specific parameters. As our understanding evolves, observational networks improve, and long-term data archives grow, we stress the need for continued development and model fidelity for high latitude terrestrial ecosystems given their importance in the global climate system.

## 5 Conclusions

Through mechanistic model development, we have reduced the biases in carbon cycling in CLM5.0 for the Arctic-Boreal PFTs. Many of our recommendations in Section 2.4 affect several of the biases noted in Section 3.1, indicative of the many interconnected schemes in CLM5.0. Ultimately, we believe our modifications to be reasonable, based in observations, and a step towards a more accurate simulation of carbon cycling in high latitude terrestrial ecosystems.

We find that a physically-based phenology formulation using soil temperatures, air temperature, and snow depth is more accurate than the existing parameterization developed for temperate latitudes. Allowing offset timing to vary with latitude instead of a single global value improved circumpolar leaf offset. We improve the scaling of day light in the maximum rate of electron transport ($J_{max}$) using the maximum day length. Additionally, we remove a global initialization of the maximum rate of electron transport ($J_{max}$) and the maximum rate of carboxylation ($V_{cmax}$) that biases prediction of these critical photosynthesis components each spring. We also recommend the Leuning (2002) temperature scaling of $J_{max}$ and $V_{cmax}$ for the ABZ, as Kattge and Knorr (2007) is not optimized for the ABZ, biasing both the maximum productivity and phenology. Finally, we adjust carbon allocation ratios for ABZ PFTs to levels that better match observations and result in more realistic simulations of GPP.

We are also interested in contributing to the improvement of the global CLM5.0 simulation. We confirm that a global simulation is possible and reasonable (Supplement Fig. S12) with these additions to the code base. Additional testing at lower latitudes, which is outside of the scope of this study, is necessary to determine the effects on the global carbon budget, particularly the change in temperature scaling from Kattge and Knorr (2007) to Leuning (2002) that would be applied globally. However, for a regional simulation of the ABZ we argue that our model improvements can be used for a more accurate simulation of the high latitudes. The modifications we implement here illustrate that previous extrapolations of temperate or even tropical observations can be problematic. We advocate for more regional ABZ focused development to ensure accuracy when implemented in global simulations, as the high latitudes are a critical component of the rapidly changing climate system.

*Code availability.* Our model recommendations are currently on Github for incorporation into the CESM master branch and CLM5.1 (https://github.com/ESCOMP/CTSM/pull/947)

*Author contributions.* LB and BMR designed the study and model development. LB performed benchmarking, model development, and validation. All authors contributed to the manuscript.

*Competing interests.* The authors declare no competing interests.

*Acknowledgements.* This work was funded by the National Aeronautics and Space Administration (NASA) Arctic-Boreal Vulnerability Experiment (ABoVE) and Carbon Cycle Science programs (NNX17AE13G).

Funding for AmeriFlux data resources was provided by the U.S. Department of Energy's Office of Science. This work used eddy covariance data acquired and shared by the FLUXNET community, including these networks: AmeriFlux, AfriFlux, AsiaFlux, CarboAfrica, CarboEuropeIP, CarboItaly, CarboMont, ChinaFlux, Fluxnet-Canada, GreenGrass, ICOS, KoFlux, LBA, NECC, OzFlux-TERN, TCOS-Siberia, and USCCC. The ERA-Interim reanalysis data are provided by ECMWF and processed by LSCE. The FLUXNET eddy covariance data processing and harmonization was carried out by the European Fluxes Database Cluster, AmeriFlux Management Project, and Fluxdata project of FLUXNET, with the support of CDIAC and ICOS Ecosystem Thematic Center, and the OzFlux, ChinaFlux and AsiaFlux offices.

We would like to thank all involved in the ILAMB project, particularly Nathan Collier, for providing a valuable resource for the community.

We would like to acknowledge high-performance computing support from Cheyenne (doi:10.5065/D6RX99HX) provided by NCAR's Computational and Information Systems Laboratory, sponsored by the National Science Foundation.

## References

Alexander, H. D. and Mack, M. C.: A canopy shift in interior Alaskan boreal forests: consequences for above-and belowground carbon and nitrogen pools during post-fire succession, Ecosystems, 19, 98–114, 2016.

Ali, A. A., Xu, C., Rogers, A., Fisher, R. A., Wullschleger, S. D., Massoud, E., Vrugt, J. A., Muss, J. D., McDowell, N. G., Fisher, J. B., et al.: A global scale mechanistic model of photosynthetic capacity (LUNA V1. 0), Geoscientific Model Development, 9, 587–606, 2016.

Amiro, B.: FLUXNET2015 CA-SF1 Saskatchewan-Western Boreal, forest burned in 1977, Tech. rep., FluxNet; University of Manitoba, 2016.

Arora, V. K. and Boer, G. J.: A parameterization of leaf phenology for the terrestrial ecosystem component of climate models, Global Change Biology, 11, 39–59, 2005.

Aurela, M.: FLUXNET2015 RU-Tks Tiksi, Tech. rep., FluxNet; Finnish Meteorological Institute-Helsinki, 2016.

Aurela, M., Tuovinen, J.-P., Hatakka, J., Lohila, A., Mäkelä, T., Rainne, J., and Lauria, T.: FLUXNET2015 FI-Sod Sodankyla, Tech. rep., FluxNet; Finnish Meteorological Institute, 2016.

Bala, G., Caldeira, K., Wickett, M., Phillips, T., Lobell, D., Delire, C., and Mirin, A.: Combined climate and carbon-cycle effects of large-scale deforestation, Proceedings of the National Academy of Sciences, 104, 6550–6555, 2007.

Bauerle, W. L., Oren, R., Way, D. A., Qian, S. S., Stoy, P. C., Thornton, P. E., Bowden, J. D., Hoffman, F. M., and Reynolds, R. F.: Photoperiodic regulation of the seasonal pattern of photosynthetic capacity and the implications for carbon cycling, Proceedings of the National Academy of Sciences, 109, 8612–8617, 2012.

Beck, P. S., Juday, G. P., Alix, C., Barber, V. A., Winslow, S. E., Sousa, E. E., Heiser, P., Herriges, J. D., and Goetz, S. J.: Changes in forest productivity across Alaska consistent with biome shift, Ecology letters, 14, 373–379, 2011.

Belshe, E., Schuur, E., Bolker, B., and Bracho, R.: Incorporating spatial heterogeneity created by permafrost thaw into a landscape carbon estimate, Journal of Geophysical Research: Biogeosciences, 117, 2012.

Biancamaria, S., Cazenave, A., Mognard, N. M., Llovel, W., and Frappart, F.: Satellite-based high latitude snow volume trend, variability and contribution to sea level over 1989/2006, Global and Planetary Change, 75, 99–107, 2011.

Black, T. A.: FLUXNET2015 CA-Obs Saskatchewan-Western Boreal, Mature Black Spruce, Tech. rep., FluxNet; The University of British Columbia, 2016.

Bonan, G. B., Pollard, D., and Thompson, S. L.: Effects of boreal forest vegetation on global climate, Nature, 359, 716–718, 1992.

Borner, A. P., Kielland, K., and Walker, M. D.: Effects of simulated climate change on plant phenology and nitrogen mineralization in Alaskan Arctic tundra, Arctic, Antarctic, and Alpine Research, 40, 27–38, 2008.

Botta, A., Viovy, N., Ciais, P., Friedlingstein, P., and Monfray, P.: A global prognostic scheme of leaf onset using satellite data, Global Change Biology, 6, 709–725, 2000.

Buchwal, A., Rachlewicz, G., Fonti, P., Cherubini, P., and Gärtner, H.: Temperature modulates intra-plant growth of Salix polaris from a high Arctic site (Svalbard), Polar Biology, 36, 1305–1318, 2013.

Callaghan, T. V., Johansson, M., Brown, R. D., Groisman, P. Y., Labba, N., Radionov, V., Barry, R. G., Bulygina, O. N., Essery, R. L., Frolov, D., et al.: The changing face of Arctic snow cover: A synthesis of observed and projected changes, Ambio, 40, 17–31, 2011.

Carroll, M. and Loboda, T.: Multi-decadal surface water dynamics in north american tundra, Remote Sensing, 9, 497, 2017.

Carroll, M. L., Townshend, J., DiMiceli, C., Loboda, T., and Sohlberg, R.: Shrinking lakes of the Arctic: Spatial relationships and trajectory of change, Geophysical Research Letters, 38, 2011.

CESM2.0: Community Earth System Model, http://www.cesm.ucar.edu/models/cesm2/, accessed 2020-03-27.

Chapin, F. S., Sturm, M., Serreze, M. C., McFadden, J. P., Key, J., Lloyd, A. H., McGuire, A., Rupp, T. S., Lynch, A. H., Schimel, J. P., et al.: Role of land-surface changes in Arctic summer warming, science, 310, 657–660, 2005.

Chapin, F. S., Woodwell, G. M., Randerson, J. T., Rastetter, E. B., Lovett, G. M., Baldocchi, D. D., Clark, D. A., Harmon, M. E., Schimel, D. S., Valentini, R., et al.: Reconciling carbon-cycle concepts, terminology, and methods, Ecosystems, 9, 1041–1050, 2006.

Chapin III, F. S.: Nutrient allocation and responses to defoliation in tundra plants, Arctic and Alpine Research, 12, 553–563, 1980.

Chapin III, F. S. and Shaver, G. R.: Physiological and growth responses of arctic plants to a field experiment simulating climatic change, Ecology, 77, 822–840, 1996.

Chen, Z., Yu, G., Zhu, X., Wang, Q., Niu, S., and Hu, Z.: Covariation between gross primary production and ecosystem respiration across space and the underlying mechanisms: a global synthesis, Agricultural and Forest Meteorology, 203, 180–190, 2015.

Ciais, P., Tans, P., Trolier, M., White, J., and Francey, R.: A large northern hemisphere terrestrial CO2 sink indicated by the 13C/12C ratio of atmospheric CO2, Science, 269, 1098–1102, 1995.

Collier, N., Hoffman, F. M., Lawrence, D. M., Keppel-Aleks, G., Koven, C. D., Riley, W. J., Mu, M., and Randerson, J. T.: The International Land Model Benchmarking (ILAMB) system: design, theory, and implementation, Journal of Advances in Modeling Earth Systems, 10, 2731–2754, 2018.

Commane, R., Lindaas, J., Benmergui, J., Luus, K. A., Chang, R. Y.-W., Daube, B. C., Euskirchen, E. S., Henderson, J. M., Karion, A., Miller, J. B., Parazoo, N. C., Randerson, J. T., Sweeney, C., Tans, P., Thoning, K., Veraverbeke, S., Miller, C. E., and Wofsy, S. C.: Carbon dioxide sources from Alaska driven by increasing early winter respiration from Arctic tundra, Proceedings of the National Academy of Sciences, 114, 5361–5366, 2017.

Computational and Laboratory, I. S.: Cheyenne: HPE/SGI ICE XA System (University Community Computing), doi:10.5065/D6RX99HX, 2017.

Corradi, C., Kolle, O., Walter, K., Zimov, S., and Schulze, E.-D.: Carbon dioxide and methane exchange of a north-east Siberian tussock tundra, Global Change Biology, 11, 1910–1925, 2005.

Duncan, B. N., Ott, L. E., Abshire, J. B., Brucker, L., Carroll, M. L., Carton, J., Comiso, J. C., Dinnat, E. P., Forbes, B. C., Gonsamo, A., et al.: Space-Based Observations for Understanding Changes in the Arctic-Boreal Zone, Reviews of Geophysics, 58, e2019RG000 652, 2020.

Eitel, J. U., Maguire, A. J., Boelman, N., Vierling, L. A., Griffin, K. L., Jensen, J., Magney, T. S., Mahoney, P. J., Meddens, A. J., Silva, C., et al.: Proximal remote sensing of tree physiology at northern treeline: Do late-season changes in the photochemical reflectance index (PRI) respond to climate or photoperiod?, Remote sensing of environment, 221, 340–350, 2019.

Elmendorf, S. C., Henry, G. H., Hollister, R. D., Björk, R. G., Bjorkman, A. D., Callaghan, T. V., Collier, L. S., Cooper, E. J., Cornelissen, J. H., Day, T. A., et al.: Global assessment of experimental climate warming on tundra vegetation: heterogeneity over space and time, Ecology letters, 15, 164–175, 2012.

Euskirchen, E. S., Edgar, C., Turetsky, M., Waldrop, M. P., and Harden, J. W.: Differential response of carbon fluxes to climate in three peatland ecosystems that vary in the presence and stability of permafrost, Journal of Geophysical Research: Biogeosciences, 119, 1576–1595, 2014.

Eyring, V., Bony, S., Meehl, G. A., Senior, C. A., Stevens, B., Stouffer, R. J., and Taylor, K. E.: Overview of the Coupled Model Intercomparison Project Phase 6 (CMIP6) experimental design and organization, Geoscientific Model Development (Online), 9, 2016.

Fisher, J., Sikka, M., Oechel, W., Huntzinger, D. N., Melton, J., Koven, C., Ahlström, A., Arain, A., Baker, I., Chen, J., et al.: Carbon cycle uncertainty in the Alaskan Arctic, Biogeosciences, 11, 4271–4288, 2014.

Fisher, R. A., Wieder, W. R., Sanderson, B. M., Koven, C. D., Oleson, K. W., Xu, C., Fisher, J., Shi, M., Walker, A. P., and Lawrence, D. M.: Parametric controls on vegetation responses to biogeochemical forcing in the CLM5, Journal of Advances in Modeling Earth Systems, 2019.

Forkel, M., Carvalhais, N., Rödenbeck, C., Keeling, R., Heimann, M., Thonicke, K., Zaehle, S., and Reichstein, M.: Enhanced seasonal CO2 exchange caused by amplified plant productivity in northern ecosystems, Science, 351, 696–699, 2016.

Franklin, O., Johansson, J., Dewar, R. C., Dieckmann, U., McMurtrie, R. E., Brännström, Å., and Dybzinski, R.: Modeling carbon allocation in trees: a search for principles, Tree Physiology, 32, 648–666, 2012.

Friedlingstein, P., Joel, G., Field, C. B., and Fung, I. Y.: Toward an allocation scheme for global terrestrial carbon models, Global Change Biology, 5, 755–770, 1999.

Goulden, M., Wofsy, S., Harden, J., Trumbore, S. E., Crill, P., Gower, S., Fries, T., Daube, B., Fan, S.-M., Sutton, D., et al.: Sensitivity of boreal forest carbon balance to soil thaw, Science, 279, 214–217, 1998.

Gower, S., Vogel, J., Norman, J., Kucharik, C., Steele, S., and Stow, T.: Carbon distribution and aboveground net primary production in aspen, jack pine, and black spruce stands in Saskatchewan and Manitoba, Canada, Journal of Geophysical Research: Atmospheres, 102, 29 029–29 041, 1997.

Gower, S., Krankina, O., Olson, R., Apps, M., Linder, S., and Wang, C.: Net primary production and carbon allocation patterns of boreal forest ecosystems, Ecological applications, 11, 1395–1411, 2001.

Graven, H., Keeling, R., Piper, S., Patra, P., Stephens, B., Wofsy, S., Welp, L., Sweeney, C., Tans, P., Kelley, J., et al.: Enhanced seasonal exchange of CO2 by northern ecosystems since 1960, Science, 341, 1085–1089, 2013.

Hanes, C. C., Wang, X., Jain, P., Parisien, M.-A., Little, J. M., and Flannigan, M. D.: Fire-regime changes in Canada over the last half century, Canadian Journal of Forest Research, 49, 256–269, 2019.

Holl, D., Wille, C., Sachs, T., Schreiber, P., Runkle, B. R., Beckebanze, L., Langer, M., Boike, J., Pfeiffer, E.-M., Fedorova, I., et al.: A long-term (2002 to 2017) record of closed-path and open-path eddy covariance CO 2 net ecosystem exchange fluxes from the Siberian Arctic, Earth System Science Data, 11, 221–240, 2019.

Huntzinger, D. N., Schwalm, C., Michalak, A., Schaefer, K., King, A., Wei, Y., Jacobson, A., Liu, S., Cook, R., Post, W., et al.: The north american carbon program multi-scale synthesis and terrestrial model intercomparison project–part 1: Overview and experimental design, Geoscientific Model Development, 6, 2121–2133, 2013.

Ito, A., Inatomi, M., Huntzinger, D. N., Schwalm, C., Michalak, A. M., Cook, R., King, A. W., Mao, J., Wei, Y., Post, W. M., et al.: Decadal trends in the seasonal-cycle amplitude of terrestrial CO2 exchange resulting from the ensemble of terrestrial biosphere models, Tellus B: Chemical and Physical Meteorology, 68, 28 968, 2016.

Iversen, C. M., Sloan, V. L., Sullivan, P. F., Euskirchen, E. S., McGuire, A. D., Norby, R. J., Walker, A. P., Warren, J. M., and Wullschleger, S. D.: The unseen iceberg: plant roots in arctic tundra, New Phytologist, 205, 34–58, 2015.

Jeong, S.-J., Bloom, A. A., Schimel, D., Sweeney, C., Parazoo, N. C., Medvigy, D., Schaepman-Strub, G., Zheng, C., Schwalm, C. R., Huntzinger, D. N., et al.: Accelerating rates of Arctic carbon cycling revealed by long-term atmospheric CO2 measurements, Science advances, 4, eaao1167, 2018.

Jung, M., Reichstein, M., Schwalm, C. R., Huntingford, C., Sitch, S., Ahlström, A., Arneth, A., Camps-Valls, G., Ciais, P., Friedlingstein, P., et al.: Compensatory water effects link yearly global land CO 2 sink changes to temperature, Nature, 541, 516, 2017.

Jung, M., Schwalm, C., Migliavacca, M., Walther, S., Camps-Valls, G., Koirala, S., Anthoni, P., Besnard, S., Bodesheim, P., Carvalhais, N., et al.: Scaling carbon fluxes from eddy covariance sites to globe: Synthesis and evaluation of the FLUXCOM approach, Biogeosciences Discussions, 2019.

Kajimoto, T., Matsuura, Y., Sofronov, M., Volokitina, A., Mori, S., Osawa, A., and Abaimov, A.: Above-and belowground biomass and net primary productivity of a Larix gmelinii stand near Tura, central Siberia, Tree physiology, 19, 815–822, 1999.

Kalnay, E., Kanamitsu, M., Kistler, R., Collins, W., Deaven, D., Gandin, L., Iredell, M., Saha, S., White, G., Woollen, J., et al.: The NCEP/NCAR 40-year reanalysis project, Bulletin of the American meteorological Society, 77, 437–471, 1996.

Kasischke, E. S., Verbyla, D. L., Rupp, T. S., McGuire, A. D., Murphy, K. A., Jandt, R., Barnes, J. L., Hoy, E. E., Duffy, P. A., Calef, M., et al.: Alaska's changing fire regime—implications for the vulnerability of its boreal forests, Canadian Journal of Forest Research, 40, 1313–1324, 2010.

Kattge, J. and Knorr, W.: Temperature acclimation in a biochemical model of photosynthesis: a reanalysis of data from 36 species, Plant, cell & environment, 30, 1176–1190, 2007.

Keeling, C. D., Chin, J., and Whorf, T.: Increased activity of northern vegetation inferred from atmospheric CO2 measurements, Nature, 382, 146, 1996.

Kennedy, D., Swenson, S., Oleson, K. W., Lawrence, D. M., Fisher, R., Lola da Costa, A. C., and Gentine, P.: Implementing plant hydraulics in the community land model, version 5, Journal of Advances in Modeling Earth Systems, 11, 485–513, 2019.

Kim, Y., Kimball, J. S., Zhang, K., and McDonald, K. C.: Satellite detection of increasing Northern Hemisphere non-frozen seasons from 1979 to 2008: Implications for regional vegetation growth, Remote Sensing of Environment, 121, 472–487, 2012.

Kobak, K., Turcmnovich, I. Y., Kondrasiheva, N. Y., Schulze, E.-D., Schulze, W., Koch, H., and Vygodskaya, N.: Vulnerability and adaptation of the larch forest in eastern Siberia to climate change, Water, Air, and Soil Pollution, 92, 119–127, 1996.

Koven, C. D., Lawrence, D. M., and Riley, W. J.: Permafrost carbon- climate feedback is sensitive to deep soil carbon decomposability but not deep soil nitrogen dynamics, Proceedings of the National Academy of Sciences, 112, 3752–3757, 2015.

Kumarathunge, D. P., Medlyn, B. E., Drake, J. E., Tjoelker, M. G., Aspinwall, M. J., Battaglia, M., Cano, F. J., Carter, K. R., Cavaleri, M. A., Cernusak, L. A., et al.: Acclimation and adaptation components of the temperature dependence of plant photosynthesis at the global scale, New Phytologist, 222, 768–784, 2019.

Kutzbach, L., Sachs, T., Boike, J., Wille, C., Schreiber, P., Langer, M., and Pfeiffer, E.-M.: FLUXNET2015 RU-Sam Samoylov, Tech. rep., FluxNet; GFZ German Research Centre for Geosciences, https://doi.org/10.18140/FLX/1440185, 2002-2014.

Lamarque, J.-F., Bond, T. C., Eyring, V., Granier, C., Heil, A., Klimont, Z., Lee, D., Liousse, C., Mieville, A., Owen, B., et al.: Historical (1850–2000) gridded anthropogenic and biomass burning emissions of reactive gases and aerosols: methodology and application, 2010.

Lawrence, D. M., Hurtt, G. C., Arneth, A., Brovkin, V., Calvin, K. V., Jones, A. D., Jones, C. D., Lawrence, P. J., de Noblet-Ducoudré, N., Pongratz, J., et al.: The Land Use Model Intercomparison Project (LUMIP) contribution to CMIP6: rationale and experimental design, Geoscientific Model Development, 9, 2973–2998, 2016.

Lawrence, D. M., Fisher, R. A., Koven, C. D., Oleson, K. W., Swenson, S. C., Bonan, G., Collier, N., Ghimire, B., van Kampenhout, L., Kennedy, D., et al.: The Community Land Model version 5: Description of new features, benchmarking, and impact of forcing uncertainty, Journal of Advances in Modeling Earth Systems, 2019.

Leuning, R.: Temperature dependence of two parameters in a photosynthesis model, Plant, Cell & Environment, 25, 1205–1210, 2002.

Li, H., Wigmosta, M. S., Wu, H., Huang, M., Ke, Y., Coleman, A. M., and Leung, L. R.: A physically based runoff routing model for land surface and earth system models, Journal of Hydrometeorology, 14, 808–828, 2013.

Lin, X., Rogers, B. M., Sweeney, C., Chevallier, F., Arshinov, M., Dlugokencky, E., Machida, T., Sasakawa, M., Tans, P., and Keppel-Aleks, G.: Siberian and temperate ecosystems shape Northern Hemisphere atmospheric CO2 seasonal amplification, Proceedings of the National Academy of Sciences, 117, 21 079–21 087, 2020.

Liptak, J., Keppel-Aleks, G., and Lindsay, K.: Drivers of multi-century trends in the atmospheric CO 2 mean annual cycle in a prognostic ESM, Biogeosciences, 14, 1383–1401, 2017.

Lloyd, A. H. and Fastie, C. L.: Recent changes in treeline forest distribution and structure in interior Alaska, Ecoscience, 10, 176–185, 2003.

Marchand, F. L., Nijs, I., Heuer, M., Mertens, S., Kockelbergh, F., Pontailler, J.-Y., Impens, I., and Beyens, L.: Climate warming postpones senescence in High Arctic tundra, Arctic, Antarctic, and Alpine Research, 36, 390–394, 2004.

Margolis, H.: AmeriFlux CA-Qc2 Quebec-1975 Harvested Black Spruce (HBS75), Tech. rep., AmeriFlux; Laval University, 2018.

Maximov, T.: FLUXNET2015 RU-SkP Yakutsk Spasskaya Pad larch, Tech. rep., FluxNet; IBPC, Russia, 2016.

McCaughey, H.: FLUXNET2015 CA-Gro Ontario-Groundhog River, Boreal Mixedwood Forest, Tech. rep., FluxNet; Queen's University, 2016.

McGuire, A., Hayes, D. J., Kicklighter, D. W., Manizza, M., Zhuang, Q., Chen, M., Follows, M. J., Gurney, K., Mcclelland, J. W., Melillo, J., et al.: An analysis of the carbon balance of the Arctic Basin from 1997 to 2006, Tellus B: Chemical and Physical Meteorology, 62, 455–474, 2010.

McGuire, A. D., Anderson, L. G., Christensen, T. R., Dallimore, S., Guo, L., Hayes, D. J., Heimann, M., Lorenson, T. D., Macdonald, R. W., and Roulet, N.: Sensitivity of the carbon cycle in the Arctic to climate change, Ecological Monographs, 79, 523–555, 2009.

McGuire, A. D., Lawrence, D. M., Koven, C., Clein, J. S., Burke, E., Chen, G., Jafarov, E., MacDougall, A. H., Marchenko, S., Nicolsky, D., et al.: Dependence of the evolution of carbon dynamics in the northern permafrost region on the trajectory of climate change, Proceedings of the National Academy of Sciences, 115, 3882–3887, 2018.

McMILLAN, A. M., Winston, G. C., and Goulden, M. L.: Age-dependent response of boreal forest to temperature and rainfall variability, Global Change Biology, 14, 1904–1916, 2008.

Medlyn, B. E., Duursma, R. A., Eamus, D., Ellsworth, D. S., Prentice, I. C., Barton, C. V., Crous, K. Y., De Angelis, P., Freeman, M., and Wingate, L.: Reconciling the optimal and empirical approaches to modelling stomatal conductance, Global Change Biology, 17, 2134–2144, 2011.

Montané, F., Fox, A. M., Arellano, A. F., MacBean, N., Alexander, M. R., Dye, A., Bishop, D. A., Trouet, V., Babst, F., Hessl, A. E., et al.: Evaluating the effect of alternative carbon allocation schemes in a land surface model (CLM4. 5) on carbon fluxes, pools, and turnover in temperate forests, Geoscientific Model Development (Online), 10, 2017.

Myers-Smith, I. H., Forbes, B. C., Wilmking, M., Hallinger, M., Lantz, T., Blok, D., Tape, K. D., Macias-Fauria, M., Sass-Klaassen, U., Lévesque, E., et al.: Shrub expansion in tundra ecosystems: dynamics, impacts and research priorities, Environmental Research Letters, 6, 045 509, 2011.

Myers-Smith, I. H., Elmendorf, S. C., Beck, P. S., Wilmking, M., Hallinger, M., Blok, D., Tape, K. D., Rayback, S. A., Macias-Fauria, M., Forbes, B. C., et al.: Climate sensitivity of shrub growth across the tundra biome, Nature Climate Change, 5, 887–891, 2015.

Natali, S. M., Schuur, E. A., Webb, E. E., Pries, C. E. H., and Crummer, K. G.: Permafrost degradation stimulates carbon loss from experimentally warmed tundra, Ecology, 95, 602–608, 2014.

Natali, S. M., Watts, J. D., Rogers, B. M., Potter, S., Ludwig, S. M., Selbmann, A. K., Sullivan, P. F., Abbott, B. W., Arndt, K. A., Birch, L., et al.: Large loss of CO 2 in winter observed across the northern permafrost region, Nature Climate Change, 9, 852–857, 2019.

Negrón-Juárez, R. I., Koven, C. D., Riley, W. J., Knox, R. G., and Chambers, J. Q.: Observed allocations of productivity and biomass, and turnover times in tropical forests are not accurately represented in CMIP5 Earth system models, Environmental Research Letters, 10, 064 017, 2015.

Oberbauer, S., Elmendorf, S., Troxler, T., Hollister, R., Rocha, A., Bret-Harte, M., Dawes, M., Fosaa, A., Henry, G., Høye, T. T., et al.: Phenological response of tundra plants to background climate variation tested using the International Tundra Experiment, Philosophical Transactions of the Royal Society B: Biological Sciences, 368, 20120 481, 2013.

Oechel, W. C., Laskowski, C. A., Burba, G., Gioli, B., and Kalhori, A. A.: Annual patterns and budget of CO2 flux in an Arctic tussock tundra ecosystem, Journal of Geophysical Research: Biogeosciences, 119, 323–339, 2014.

Parazoo, N. C., Koven, C. D., Lawrence, D. M., Romanovsky, V., and Miller, C. E.: Detecting the permafrost carbon feedback: talik formation and increased cold-season respiration as precursors to sink-to-source transitions, The Cryosphere (Online), 12, 2018.

Peng, S., Ciais, P., Chevallier, F., Peylin, P., Cadule, P., Sitch, S., Piao, S., Ahlström, A., Huntingford, C., Levy, P., et al.: Benchmarking the seasonal cycle of CO2 fluxes simulated by terrestrial ecosystem models, Global Biogeochemical Cycles, 29, 46–64, 2015.

Phoenix, G. K. and Bjerke, J. W.: Arctic browning: extreme events and trends reversing arctic greening, Global Change Biology, 22, 2960–2962, 2016.

Piao, S., Ciais, P., Friedlingstein, P., Peylin, P., Reichstein, M., Luyssaert, S., Margolis, H., Fang, J., Barr, A., Chen, A., et al.: Net carbon dioxide losses of northern ecosystems in response to autumn warming, Nature, 451, 49–52, 2008.

Piao, S., Sitch, S., Ciais, P., Friedlingstein, P., Peylin, P., Wang, X., Ahlström, A., Anav, A., Canadell, J. G., Cong, N., et al.: Evaluation of terrestrial carbon cycle models for their response to climate variability and to CO2 trends, Global change biology, 19, 2117–2132, 2013.

Randerson, J., Field, C., Fung, I., and Tans, P.: Increases in early season ecosystem uptake explain recent changes in the seasonal cycle of atmospheric CO2 at high northern latitudes, Geophysical Research Letters, 26, 2765–2768, 1999.

Randerson, J. T., Thompson, M. V., Conway, T. J., Fung, I. Y., and Field, C. B.: The contribution of terrestrial sources and sinks to trends in the seasonal cycle of atmospheric carbon dioxide, Global Biogeochemical Cycles, 11, 535–560, 1997.

Richardson, A. D., Anderson, R. S., Arain, M. A., Barr, A. G., Bohrer, G., Chen, G., Chen, J. M., Ciais, P., Davis, K. J., Desai, A. R., et al.: Terrestrial biosphere models need better representation of vegetation phenology: results from the N orth A merican C arbon P rogram S ite S ynthesis, Global Change Biology, 18, 566–584, 2012.

Rogers, A., Serbin, S. P., Ely, K. S., Sloan, V. L., and Wullschleger, S. D.: Terrestrial biosphere models underestimate photosynthetic capacity and CO2 assimilation in the Arctic, New Phytologist, 216, 1090–1103, 2017.

Rogers, B., Randerson, J., and Bonan, G.: High-latitude cooling associated with landscape changes from North American boreal forest fires, Biogeosciences, 10, 699–718, 2013.

Rogers, B. M., Soja, A. J., Goulden, M. L., and Randerson, J. T.: Influence of tree species on continental differences in boreal fires and climate feedbacks, Nature Geoscience, 8, 228–234, 2015.

Rogers, B. M., Solvik, K., Hogg, E. H., Ju, J., Masek, J. G., Michaelian, M., Berner, L. T., and Goetz, S. J.: Detecting early warning signals of tree mortality in boreal North America using multiscale satellite data, Global change biology, 24, 2284–2304, 2018.

Runkle, B. R., Sachs, T., Wille, C., Pfeiffer, E.-M., and Kutzbach, L.: Bulk partitioning the growing season net ecosystem exchange of CO 2 in Siberian tundra reveals the seasonality of its carbon sequestration strength., Biogeosciences, 10, 2013.

Salmon, V. G., Soucy, P., Mauritz, M., Celis, G., Natali, S. M., Mack, M. C., and Schuur, E. A.: Nitrogen availability increases in a tundra ecosystem during five years of experimental permafrost thaw, Global Change Biology, 22, 1927–1941, 2016.

Schaefer, K., Schwalm, C. R., Williams, C., Arain, M. A., Barr, A., Chen, J. M., Davis, K. J., Dimitrov, D., Hilton, T. W., Hollinger, D. Y., et al.: A model-data comparison of gross primary productivity: Results from the North American Carbon Program site synthesis, Journal of Geophysical Research: Biogeosciences, 117, 2012.

Schwalm, C. R., Williams, C. A., Schaefer, K., Anderson, R., Arain, M. A., Baker, I., Barr, A., Black, T. A., Chen, G., Chen, J. M., et al.: A model-data intercomparison of CO2 exchange across North America: Results from the North American Carbon Program site synthesis, Journal of Geophysical Research: Biogeosciences, 115, 2010.

Searle, E. B. and Chen, H. Y.: Persistent and pervasive compositional shifts of western boreal forest plots in Canada, Global Change Biology, 23, 857–866, 2017.

Serreze, M. C. and Barry, R. G.: Processes and impacts of Arctic amplification: A research synthesis, Global and planetary change, 77, 85–96, 2011.

Serreze, M. C. and Francis, J. A.: The Arctic amplification debate, Climatic change, 76, 241–264, 2006.

Shaver, G. R., Billings, W. D., Chapin III, F. S., Giblin, A. E., Nadelhoffer, K. J., Oechel, W. C., and Rastetter, E.: Global change and the carbon balance of arctic ecosystems: Carbon/nutrient interactions should act as major constraints on changes in global terrestrial carbon cycling, Bioscience, 42, 433–441, 1992.

Sloan, V. L., Fletcher, B. J., Press, M. C., Williams, M., and Phoenix, G. K.: Leaf and fine root carbon stocks and turnover are coupled across Arctic ecosystems, Global Change Biology, 19, 3668–3676, 2013.

Smith, N. G., Lombardozzi, D., Tawfik, A., Bonan, G., and Dukes, J. S.: Biophysical consequences of photosynthetic temperature acclimation for climate, Journal of Advances in Modeling Earth Systems, 9, 536–547, 2017.

Starr, G. and Oberbauer, S. F.: Photosynthesis of arctic evergreens under snow: implications for tundra ecosystem carbon balance, Ecology, 84, 1415–1420, 2003.

Stöckli, R., Lawrence, D., Niu, G.-Y., Oleson, K., Thornton, P. E., Yang, Z.-L., Bonan, G., Denning, A., and Running, S. W.: Use of FLUXNET in the Community Land Model development, Journal of Geophysical Research: Biogeosciences, 113, 2008.

Sulla-Menashe, D. and Friedl, M. A.: MCD12Q1 MODIS/Terra+Aqua Land Cover Type Yearly L3 Global 500m SIN Grid V006, DOI: 10.5067/MODIS/MCD12Q1.006, accessed 2020-03-27, 2019.

Taylor, K. E., Stouffer, R. J., and Meehl, G. A.: An overview of CMIP5 and the experiment design, Bulletin of the American Meteorological Society, 93, 485–498, 2012.

Tramontana, G., Jung, M., Camps-Valls, G., Ichii, K., Ráduly, B., Reichstein, M., Schwalm, C. R., Arain, M. A., Cescatti, A., Kiely, G., et al.: Predicting carbon dioxide and energy fluxes across global FLUXNET sites with regression algorithms, Biogeosciences Discussions, 2016.

Turetsky, M. R., Kane, E. S., Harden, J. W., Ottmar, R. D., Manies, K. L., Hoy, E., and Kasischke, E. S.: Recent acceleration of biomass burning and carbon losses in Alaskan forests and peatlands, Nature Geoscience, 4, 27–31, 2011.

Van den Hurk, B., Kim, H., Krinner, G., Seneviratne, S. I., Derksen, C., Oki, T., Douville, H., Colin, J., Ducharne, A., Cheruy, F., et al.: LS3MIP (v1. 0) contribution to CMIP6: the Land Surface, Snow and Soil moisture Model Intercomparison Project-aims, setup and expected outcome, Geoscientific Model Development, 9, 2809–2832, 2016.

Vanninen, P. and Mäkelä, A.: Carbon budget for Scots pine trees: effects of size, competition and site fertility on growth allocation and production, Tree Physiology, 25, 17–30, 2005.

Verbyla, D.: Browning boreal forests of western North America, Environmental Research Letters, 6, 041 003, 2011.

Virkkala, A.-M., Virtanen, T., Lehtonen, A., Rinne, J., and Luoto, M.: The current state of CO2 flux chamber studies in the Arctic tundra: A review, Progress in Physical Geography: Earth and Environment, 42, 162–184, 2018.

Virkkala, A.-M., Abdi, A. M., Luoto, M., and Metcalfe, D. B.: Identifying multidisciplinary research gaps across Arctic terrestrial gradients, Environmental Research Letters, 14, 124 061, 2019.

Walker, X. and Johnstone, J. F.: Widespread negative correlations between black spruce growth and temperature across topographic moisture gradients in the boreal forest, Environmental Research Letters, 9, 064 016, 2014.

Walker, X. J., Mack, M. C., and Johnstone, J. F.: Stable carbon isotope analysis reveals widespread drought stress in boreal black spruce forests, Global Change Biology, 21, 3102–3113, 2015.

Welp, L. R., Patra, P. K., Rödenbeck, C., Nemani, R., Bi, J., Piper, S. C., and Keeling, R. F.: Increasing summer net CO2 uptake in high northern ecosystems inferred from atmospheric inversions and comparisons to remote-sensing NDVI, Atmospheric Chemistry and Physics, 16, 9047–9066, 2016.

White, M. A., Thornton, P. E., and Running, S. W.: A continental phenology model for monitoring vegetation responses to interannual climatic variability, Global biogeochemical cycles, 11, 217–234, 1997.

White, M. A., de Beurs, K. M., Didan, K., Inouye, D. W., Richardson, A. D., Jensen, O. P., O'KEEFE, J., Zhang, G., Nemani, R. R., van Leeuwen, W. J., et al.: Intercomparison, interpretation, and assessment of spring phenology in North America estimated from remote sensing for 1982–2006, Global Change Biology, 15, 2335–2359, 2009.

Wieder, W. R., Lawrence, D. M., Fisher, R. A., Bonan, G. B., Cheng, S. J., Goodale, C. L., Grandy, A. S., Koven, C. D., Lombardozzi, D. L., Oleson, K. W., et al.: Beyond static benchmarking: Using experimental manipulations to evaluate land model assumptions, Global Biogeochemical Cycles, 2019.

Zhang, X., Friedl, M. A., Schaaf, C. B., and Strahler, A. H.: Climate controls on vegetation phenological patterns in northern mid-and high latitudes inferred from MODIS data, Global change biology, 10, 1133–1145, 2004.

Zhao, F. and Zeng, N.: Continued increase in atmospheric CO 2 seasonal amplitude in the 21st century projected by the CMIP5 Earth system models, Earth System Dynamics, 5, 423–439, 2014.

Zhao, F., Zeng, N., Asrar, G., Friedlingstein, P., Ito, A., Jain, A., Kalnay, E., Kato, E., Koven, C., Poulter, B., et al.: Role of CO2, climate and land use in regulating the seasonal amplitude increase of carbon fluxes in terrestrial ecosystems: a multimodel analysis, Biogeosciences, 13, 5121–5137, 2016.

Zimov, S., Davidov, S., Voropaev, Y. V., Prosiannikov, S., Semiletov, I., Chapin, M., and Chapin, F.: Siberian CO 2 efflux in winter as a CO 2 source and cause of seasonality in atmospheric CO 2, Climatic Change, 33, 111–120, 1996.

Zimov, S., Davidov, S., Zimova, G., Davidova, A., Chapin, F., Chapin, M., and Reynolds, J.: Contribution of disturbance to increasing seasonal amplitude of atmospheric CO2, Science, 284, 1973–1976, 1999.